MISSOURI S&T

CENTER FOR TRANSPORTATION INFRASTRUCTURE AND SAFETY

Admixture Compatibility of Alternative Supplementary Cementitious Materials for Pavement and Structural Concrete

by

Ehsan Ghafari[1], Aasiyah Baig[2], Kevin Nicoletta[2], Dimitri Feys[1], Raissa Douglas Ferron[2] and Kamal H. Khayat[1]

[1]Civil, Architectural and Environmental Engineering Department
Missouri University of Science and Technology, Rolla, MO, United States
[2]Civil, Architectural and Environmental Engineering Department
University of Texas at Austin, Austin, TX, United States

August 2014

A National University Transportation Center at Missouri University of Science and Technology

NUTC R366

Disclaimer

The contents of this report reflect the views of the author(s), who are responsible for the facts and the accuracy of information presented herein. This document is disseminated under the sponsorship of the Department of Transportation, University Transportation Centers Program and the Center for Transportation Infrastructure and Safety NUTC program at the Missouri University of Science and Technology, in the interest of information exchange. The U.S. Government and Center for Transportation Infrastructure and Safety assumes no liability for the contents or use thereof.

Technical Report Documentation Page

1. Report No.	2. Government Accession No.	3. Recipient's Catalog No.
NUTC R366		

4. Title and Subtitle	5. Report Date
Admixture Compatibility of Alternative Supplementary Cementitious Materials for Pavement and Structural Concrete	August 2014
	6. Performing Organization Code

7. Author/s	8. Performing Organization Report No.
Ehsan Ghafari, Aasiyah Baig, Kevin Nicoletta, Dimitri Feys, Raissa Douglas Ferron and Kamal H. Khayat	Project #0043315

9. Performing Organization Name and Address	10. Work Unit No. (TRAIS)
Center for Transportation Infrastructure and Safety/NUTC program Missouri University of Science and Technology 220 Engineering Research Lab Rolla, MO 65409	11. Contract or Grant No. DTRT06-G-0014

12. Sponsoring Organization Name and Address	13. Type of Report and Period Covered
U.S. Department of Transportation Research and Innovative Technology Administration 1200 New Jersey Avenue, SE Washington, DC 20590	Final
	14. Sponsoring Agency Code

15. Supplementary Notes

16. Abstract

The objectives of this research project were: (1) to gain a better understanding about the interaction among alternative SCMS and chemical admixtures in Portland cement mixtures; and (2) to facilitate implementation of alternative SCMs in transportation structures. Such information can assist in the encouraging adoption of alternative SCMs in the United States, both in pavement and structural applications. In order to accomplish these goals, the NUTC project:
(1) Investigated the influence of selected types of alternative SCMs on air-void system in concrete for pavements
(2) Investigated the influence of selected alternative SCMs on key fresh and hardened properties of concrete designated for structural applications

17. Key Words	18. Distribution Statement
Supplementary cementing materials, durability, concrete, fresh properties and mechanical properties	No restrictions. This document is available to the public through the National Technical Information Service, Springfield, Virginia 22161.

19. Security Classification (of this report)	20. Security Classification (of this page)	21. No. Of Pages	22. Price
unclassified	unclassified	60	

Form DOT F 1700.7 (8-72)

Admixture Compatibility of Alternative Supplementary Cementitious Materials for Pavement and Structural Concrete

Final Report

Ehsan Ghafari[1], Aasiyah Baig[2], Kevin Nicoletta[2], Dimitri Feys[1], Raissa Douglas Ferron[2], and Kamal H. Khayat[1]

[1]Civil, Architectural and Environmental Engineering Department, Missouri University of Science and Technology, Rolla, MO, United States

[2]Civil, Architectural and Environmental Engineering Department, University of Texas at Austin, Austin, TX, United States

The authors would like to acknowledge the US Department of Transportation for the financial support for the project.

1 Introduction

1.1 Literature Review

Supplementary cementitious materials (SCMs) provide many benefits to the transportation and construction industry due to the cost savings, long-term strength improvements, and enhanced durability that results from incorporting SCMs in portland cement concrete. An SCM is a material that contributes to the properties of a cementitious mixture through *hydraulic* or *pozzolanic activity*, or both. Fly ash is the most widely used SCM in United States. However concerns about the future availability of fly ash have arisen due to the implentation of pollution control devices in coal combustion plants and increased blending of powder river basin coals, both of which can influence the composition (and hence quality) of the resulting fly ash. Based on these concerns, the Texas Department of Transportation (TxDOT) has funded a research project (0-6717) that is being conducted at the University of Texas at Austin (UT-Austin). This project started in August 2011 and ends in August 2014. TxDOT 0-6717 is focused on pavement mixtures and investigates various materials (calcined shales, pumice, perlite, diatomaceous earth, volcanic ash, and zeolites) that could substitute fly ash and perform similarly to Class F fly ash based on pozzolanic reactivity: compressive srength, workability, drying shrinkage, thermal expansion properties,resistance to alkali-silica reaction, resistance to sulfate attack, and resistance to chloride ion penetration. If concrete is used in areas exposed to variations in moisture and temperature, then the effect of the fly ash alternatives to freeze-thaw resistance is also of concern. Commonly, entrained air bubbles are purposely trapped in concrete for frost resistance. The air void system of the concrete paste should be made up of generally small and uniformly spaced air voids. Many factors influence the ability to entrain and stabilize microscopic air-voids in concrete. The air-void system created by air-entraining agents (AEA) is greatly influeced by concrete materials and construction practices. Differences in cement, sand, aggregate, and other admixture compostions can cause changes in the air-void system; of particular concern is the type of SCM that is used since residual carbon on an SCM (such that is often seen in fly ashes with a high loss of ignitition (LOI) value) can impair the air-void system. Since the use of chemical and mineral admixtures has become common practice the interaction between these admixtures and AEA has created concern. Kleiger, Stark, and Teske [1] showed that concrete containing fly ash produced relatively stable air-void systems. However, in Pigeon and Plante [2] the volume of air entrained varied based on the chemical composition of the fly ash. The amount of AEA needed varied siginificantly based on the presence and composition of the fly ash. Pavement mixtures are typically characterized by having a lower slump and lower binder content than structural concrete mixtures. As such, structural concretes typically contain larger quantities of water-reducer or more powerful water reducers (e.g high-range water reducers) than pavement concretes. As such, examining the natural pozzolan-AEA interaction and its effect on the air void system is warrented.

All of the considered materials examined in TxDOT 0-6717 can be considered as natural pozzolans, and they were selected based on cost and availablity, with a particular focus on the availability of the material in Texas. In addition to availability of the source and cost, the composition of the material such as oxide composition, fineness, strength, and water requirement plays a large factor on the suitability of a material as an alternative SCM (herein called ASCM) since it will affect the performance of the material. The American Standard of Testing Materials (ASTM) defines a pozzolan in C 125 as a “siliceous and aluminous material that in itself possesses little or no cementious value but will, in finely divided form and in the presence of water, chemically react with calcium hydroxide at ordinary temperature to form

compounds possessing cementious properties. ASTM C 618 provides examples of natural pozzolans as diatomaceous earth, shales, clay, pumice and volcanic ash. Of the approved SCMs listed by TxDOT, metakaolin is the only natural pozzolan (the others are Class C and F fly ashes, ground-granulated blast funace slag, silica fume). Yet, in addition to metakaolin, Texas has a commercial availability of pumice, perlite, zeolites, and calcined shale. In this project, 3 of the most promising natural pozzolans that were examined in TxDOT 0-6717 were selected for further examination. These 3 pozzolans were perlite, pumice, and zeolite. A brief overview of these materials are provided below. Further details about these materials can be found in the final report of TxDOT 0-6717 when it is published.

- Perlite is a highly siliceous and amorphous hydrated volcanic glass composed of few crystalline impurities, like quartz, biotite, and alkali feldspars and falls into the category of unaltered volcanic alternative. Perlite is defined as a hydrated natural rhyolite, which is glass formed from highly siliceous volcanic lava [3]. Perlite varies from other hydrated volcanic glasses (e.g. obsidian or pumice) based on its high water content (typically ranging from 2-5%) [4]. The primary hydration of perlite takes place during the formation of the volcanic glass and additionally the second hydration occurs late in the cooling process of the glass. When perlite is heated rapidly, it expands to form a white, porous, lightweight aggregate known as expanded perlite. When heated it begins to become soft. When heated high enough the internal water boils off creating the perlite to expand as the steam escapes creating small bubbles. The siliceous content and amorphous structure of the perlite makes it an ideal candidate to be tested as pozzolan for use in concrete. A study done by Ray et al showed that mortar mixes containing perlite showed similar characteristics to mortars with traditional SCMs, fly ash and silica fume, at a replacement dosage of 10% [5]. Erdem et al [6] found that a higher water to cement ratio was needed to achieve normal consistency for pastes containing a perlite compared to a control with cement only. The same trend was observed for mortars. Additionally, Erdem et al. found that the initial and final setting times of the cementitious paste was greater than that of the control but still within the limits of ASTM C595 and C1157. According to USGS in 2011, the United States had a perlite reserve of 50 million metric tons with the majory ores in Arizona, California, Idaho, Nevada, New Mexico and Oregon.
- Pumice is a highly amorphous and porous volcanic rock with interconnected vesicles formed by extruded lava containing dissolved gases. Pumice has been used as a natural pozzolan throughout history dating back to the Romans. In the United States, the use of pumice dates back to the early 1900s. Several dams were built using pumice in during the mid-1900s [7]. The porous structure characterizes the material a low density rock with high absorption capacity and permeability. The use of pumice as an SCM has shown to increase the water demand primarily due to the interconnected vesicles in the pumice particles that can absorb and hold water [8]. The walls of the vesicles are made of a glassy structure due to the rapid cooling rate of the lava. The volume, shape and size of the vesicles are highly dependent on the chemical composition of the magma. Pumices are typically silicic due to originating from highly silicic magmas that results in a viscous lava flow that tends to hold more of the dissolved gases. Commercially mined pumice tends to come from air-borne deposits that are created from explosive eruptions that are a result of silicic magma. Pumice is a widely used SCM with known contribution to high compressive strengths. The vesicles in pumice are generally in a range from a micrometer to a centimeter in size. Pumices with interconnected vesicles have the potential for high absorption capacity and high permeability. Pumice can generally be cut or broken easily with steel tools and some can be crushed by hand. Thus the strength is highly based on the porous structure. Studies show that pumice has met all chemical requirements of ASTM C 619 along

with most physical requirements as long as the natural pumice was ground before testing [9-10]. The alkali content of pumice vary significantly based on the origin of the volcano [11]. Hossain reported that calcium hydroxide content of concrete containing pumice was lower than that of the control concrete not containing pumice [12]. Most studies have shown pumice to reduce strength, however calcined pumice generally yields higher compressive strengths compared to raw uncalcined pumice [13]. According to the 2012 US Geological Survey, 250 million to 1 billion tons of pumice are available in the western and Great Plains states. In 2011, eleven companies in the United States produced 539,000 tons of pumice through open it methods.

- Zeolite is a hydrated aluminosilicate mineral with a frame consisting of silicate and aluminate tetrahedras arranged in a ring [11]. The rings create pores or channels through the crystal with a constant diameter and a pore volume of up to 50% of the total volume [14]. The pores in zeolites contain exchangeable cations, which help to balance the net negative charge of the zeolite framework. Therefore the water molecules are held in the pores due to charge-dipole interactions. Zeolites are formed by diagenetic alteration, a physical or chemical change in deposited sediment under low temperature and pressure, of volcanic glasses by alkaline fluids [11]. Clinoptilolite is the most frequently identified zeolite mineral. Clinoptilolite is a member of the heulandite family of zeolites with a silica to aluminum ratio greater than 4 and therefore silica rich. Perraki et al. showed that cement pastes with 5-10% zeolites had a lower calcium hydroxide content than the control [15]. Zeolites have showed to have increasing compressive strength as the particle size decreases [16]. Zeolites require a high water demand for concrete due to its high surface area and porous crystalline structure. Several studies have confirmed the increased water demand from an increased dosage of zeolite in a mixture [17-19]. Additionally calcining zeolites past 300 degrees Fahrenheit has been shown to increase reactivity for use in concrete and therefore increase strength or pozzolanic reactivity considerably [20-21]. According to the USGS in 2011, the United States produces 65 thousand metric tons. Six companies in the United States mine zeolites in Arizona, California, Idaho, Nevada, New Mexico, Oregon and Texas [22].

1.2 Goals of this Research Project

The goals of the research plan are: (1) to gain a better understanding about the interaction between alternative SCMs (herein called ASCMs) and chemical admixtures in Portland cement mixtures; and (2) to facilitate implementation of alternative SCMs in transportation infrastructure. Such information can assist in the encouraging adoption of alternative SCMs in the United States, both in pavement and structural applications. In order to accomplish these goals, the NUTC supported project seeks to:

- Investigate the influence of selected types of ASCMS on the air-void system in concrete intended for pavement applications.
- Investigate the influence of selected types of alternative SCMs on key fresh and hardened properties of concrete designated for the construction of bridge and tunnel infrastructure.

1.3 Project Overview and Scope

The main objectives of Project 0-6717 are to determine the availability of alternative SCMs in Texas and to investigate the potential use for improving durability aspects of concrete. Based on the results on TxDOT project, perlite, pumice and specific sources of zeolite were retained for further investigation for this research project. More information regarding the performance of these ASCMS can be found in

Rachel Cano's thesis titled "Evaluation of Natural Pozzolans as Replacements for Class F Fly Ash in Portland Cement Concrete" [23]. While the workplan of Project 0-6717 investigates the influence of alternative SCMs on setting time, workability, early and long-term strength, drying shrinkage, resistance to alkali silica reaction, and sulfate attack resistance, it does not investigate how these alternative SCMs could influence the air-void system of the resulting concrete mixtures or the interactions of the various alternative SCMs with chemical admixtures. Furthermore, Project 0-6717 is focused on pavement mixtures, as such this research project will focus on examining the performance of the ASCMs in a structural concrete mixture, as well in a pavement mixture.

2 Materials Characterization and Properties

Project 0-6717 conducted a literature review on natural and non-traditional SCMs to identify candidate alternatives and classified the alternative materials into the following categories: (1) unaltered volcanic pozzolan, (2) altered volcanic pozzolan, and (3) sedimentary pozzolan. An altered volcanic material would go through some chemical or physical change such as calcining to make the material reactive, whereas an unaltered volcanic material would not have any chemical or physical alterations conducted. Sedimentary pozzonlans come from deposited rock of either mineral or organic particle settling and accumulation. Pumice and perlite were classified as unaltered volcanic pozzolans, whereas zeolite was considered to be an altered volcanic pozzolan. Further details about the selected materials used in this project are provided below:

2.1.1 Cement and SCMs

Table 2 summarizes the specific gravities and the specific surface area of the used materials. The surface area was measured with a Quantachrome Nove 2000 instrument using the BET (Brunauer Emmett Teller) method. The particle size distribution was measured using a Microtrac particle size analyzer. It uses a laser scattering method to determine particle size. Figure 1 shows particle size distribution of the cement and the used SCMs.

Cement – Types I and I/II cements according to ASTM C150, commercially available in TX and MO, were used in this project. The specific gravity of the cement is 3.16.

Class C fly ash – A Class C fly ash, commercially available in Missouri, was used as reference SCM for the evaluation of the compatibility of SCMs with chemical admixtures.

ASCMs – Details regarding the source, cost and current availability of ASCMs used in this project is provided in Table 1. Table 2 presents the specific gravities and surface areas of the cement, fly ash and ASCMs. Table 3 and Table 4 presents the chemical and physical analysis results of the ASCMs, and it contains information regarding the limits specified under ASTM C618 for a material to be considered a natural pozzolan. It can be seen that both the perlite and pumice meets the ASTM C618 requirements for a Class N pozzolan, however the zeolites fails moisture content, 7^{th} day strength activity index (SAI), and water requirement. The perlite and perlite used are currently sold as an SCMs. TxDOT 0-6717 examined 6 different zeolites and the zeolite selected for this project was considered to be the best overall performer of the zeolites that were examined in TxDOT 0-6717. X-ray diffraction (XRD) analysis of the zeolite, pumice and perlite was conducted as part of TxDOT 0-6717. The perlite and pumice were amorphous, whereas the zeolite was crystalline. An Si/Al ratio greater than 4 indicates the presence of clinoptilolite in zeolite, from Table 3 it can be seen that the zeolite used in this research has an Si/Al ratio that is greater than 4 and thus it is a clinoptilolite zeolite.

Table 1. Source, cost and availability of alternative natural pozzolans.

Mineral Type	**Sourced From**	**Cost**	**Availability**
Perlite	Idaho	$124/ton	Not provided
Pumice	Idaho	$116/ton	200,000 tons/year
Zeolite	Idaho	$100/ton delivered, $20-30/ton at mine site	50,000 tons/year

Table 2. Specific gravities and specific surface area (BET) of used cement and SCMs.

Materials	Specific gravity (-)	Specific Surface Area (m^2/g)
Cement	3.16	1.659
Perlite	2.37	3.172
Pumice	2.45	18.666
Fly ash class C	2.70	1.424
Zeolite	2.37	38.968

Table 3. Chemical Analysis of ASCMs and ASTM C618 limits (data obtained from Cano [23])

Material	SiO_2 (wt%)	Al_2O_3 (wt%)	Fe_2O_3 (wt%)	Sum of Oxides (wt%)	CaO (wt%)	MgO (wt%)	SO_3 (wt%)	Na_2O (wt%)	K_2O (wt%)	Moisture Content (wt%)	LOI (wt%)
Perlite	70.3	12.8	1.2	84.3	0.86	0.14	0.05	4.7	4.7	0.6	3.4
Pumice	69.4	12.4	1.1	82.9	0.94	0.44	0.04	3.8	5.2	1.5	4.4
Zeolite	65.3	10.9	2.4	78.6	2.5	0.59	0.07	0.52	4.8	5.1	2.5
ASTM C 618 Class N requirements	--	--	--	> 70.0			< 4.0			< 3.0	< 10.0

Table 4. Physical Analysis of ASCMs and ASTM C618 limits (data obtained from Cano [23])

Material	Fineness % Retained	7 day SAI % Control	28 day SAI % Control	Water Req. % Control	Soundness % Expansion
Perlite	2	86	94	100	0
Pumice	2	82	93	104	0
Zeolite	0	71	100	116	0
ASTM C 618 Class N requirements	< 34	> 75	> 75	< 115	< +/- 0.8

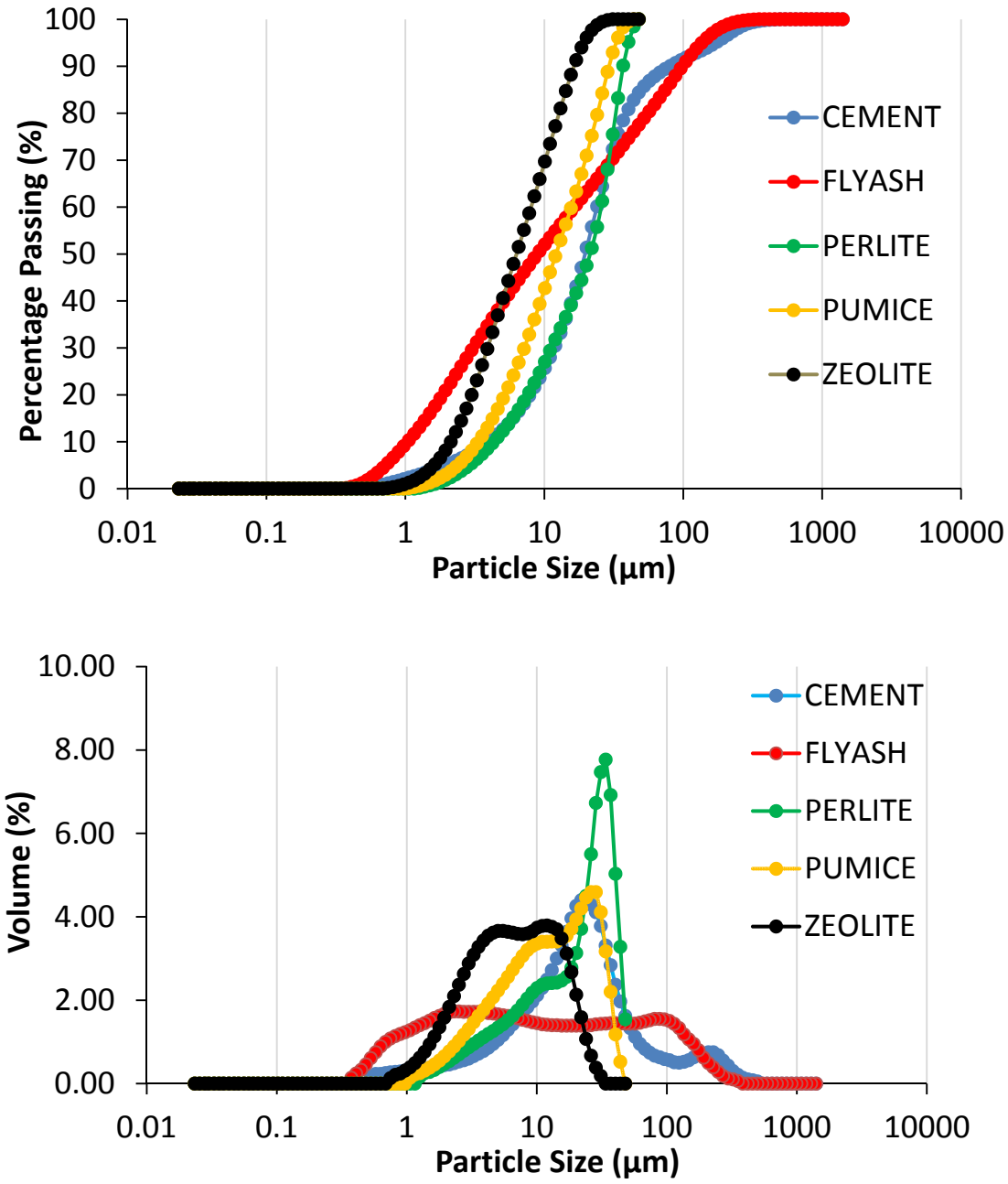

Figure 1. Particle size distribution of cement and SCMs. Top: cumulative grain size distribution, in which the cement curve is partly hidden behind the perlite curve. Bottom: grain size distribution of individual size classes, especially showing the large range of fly ash particles.

2.1.2 Chemical Admixtures

Two air-entraining admixtures (AEA) and one third generation polycarboxylate ether-based superplasticizer (SP or HRWRA) were used in this study. Both AEA met the requirements of ASTM C-260. AEA 1 is an aqueous solution of organic materials, while AEA 2 is a multi-component synthetic air-entraining agent. All chemical admixtures are commercial products available on the US market.

2.1.3 Aggregates

Coarse Aggregates for Pavement Concrete - The coarse aggregate used was a crushed, dolomitic limestone, size 57, according to ASTM C33. The specific gravity (SSD) of this aggregate was 2.56 and it had a water absorption value of 2.10% with a maximum aggregate size of 1".

Coarse Aggregates for Structural Concrete - Crushed limestone coarse aggregates with maximum aggregate size of 1/2" were used in this study. Figure 2 shows the particle size distribution of the coarse aggregates, which is in accordance with size number 7 according to ASTM C33. The aggregate has a specific gravity of 2.63 in SSD condition and a water absorption of 3.8%.

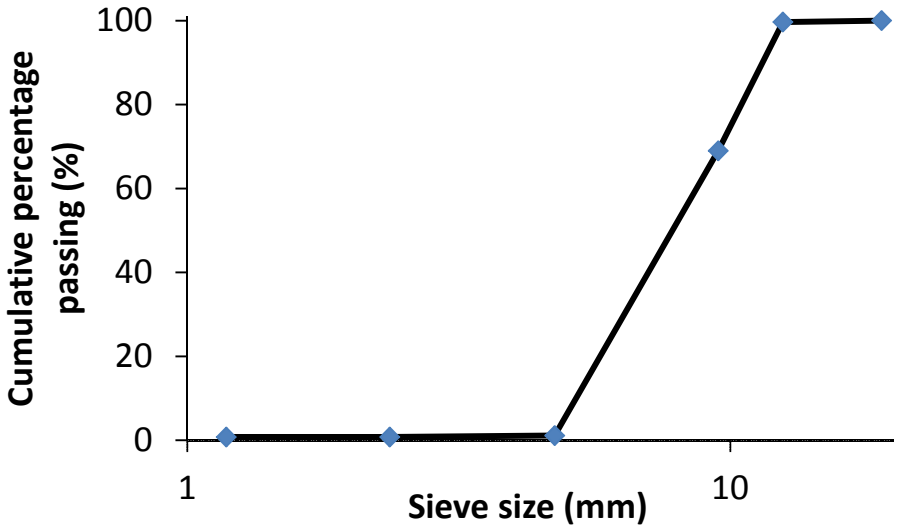

Figure 2. Grain size distribution of coarse aggregates.

Fine aggregate for Pavement Concrete - The fine aggregates used was a Colorado river sand. The specific gravity (SSD) of this aggregate was 2.62 and it had a water absorption value of 0.9%.

Fine aggregate for Structural Concrete – Missouri River sand was used as fine aggregate in this study. Figure 3 shows the gradation curve of the fine aggregates as compared to the ASTM C33 standard. The sand has a specific gravity of 2.64 and a water absorption of 0.6%.

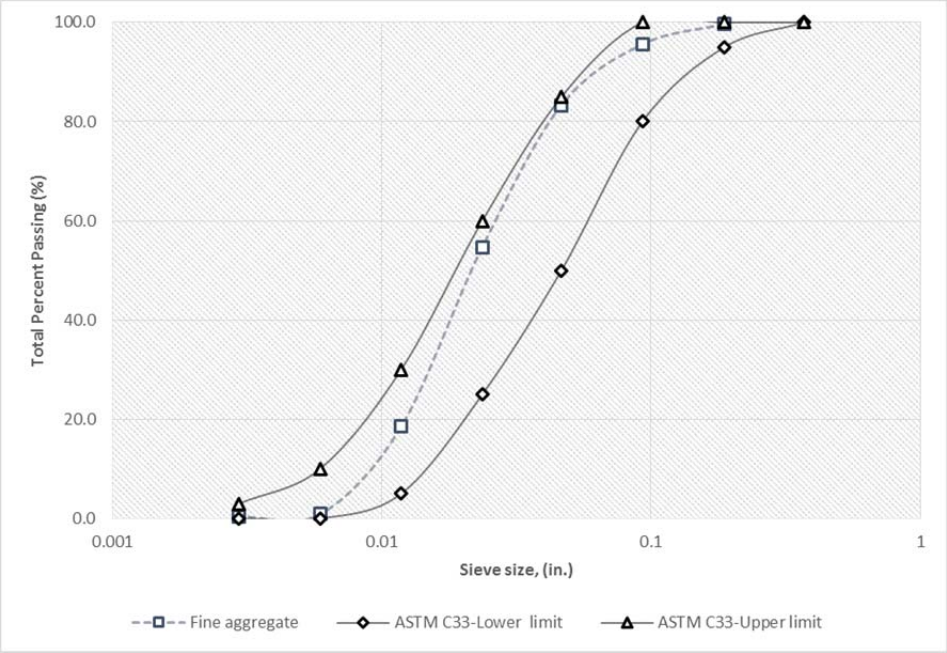

Figure 3. Grain size distribution of the employed sand, and ASTM C33 upper and lower limits.

3 Sample Preparation

3.1 Mixing Procedure

The research project involved the production of cement paste to test the saturation point, workability retention and heat of hydration. A comprehensive experimental program on concrete was conducted aiming to study the effect of different SCMs and air entrainments on the rheology, air-void system, mechanical properties and durability of concrete.

3.1.1 Mixing Procedure Cement Pastes for intended for Structural Concrete Mixtures

The mixing procedure involved the following steps using a 10 L Hobart mixer:

- All cementitious materials were premixed for 30 seconds.
- All water was added and mixed for 1 minute.
- The sides of the mixing container were scrapped for 30 seconds to ensure homogeneity of the sample.
- The mixture was blended for an additional 30 seconds, and all of the SP was slowly added.
- The mixture was blended for more two minutes.

3.1.2 Mixing Procedure for Structural Concrete Mixture

A high-shear concrete mixer (see Figure 4) with a maximum output capacity of 150 L was used to produce the concrete mixtures. The mixing procedure involved the following steps. The rotor speed and the pan speed were 4 m/s and 11 rpm, respectively.

- All aggregates were pre-mixed for 30 seconds
- The air entrainment admixture with half of the water was added to the aggregate and was mixed for 1 minute.
- The cementitious materials were added to the aggregate along with the second half of the mixing water, and the material was mixed for 30 seconds.
- The SP was added, and the mixture was blended for final two minutes.

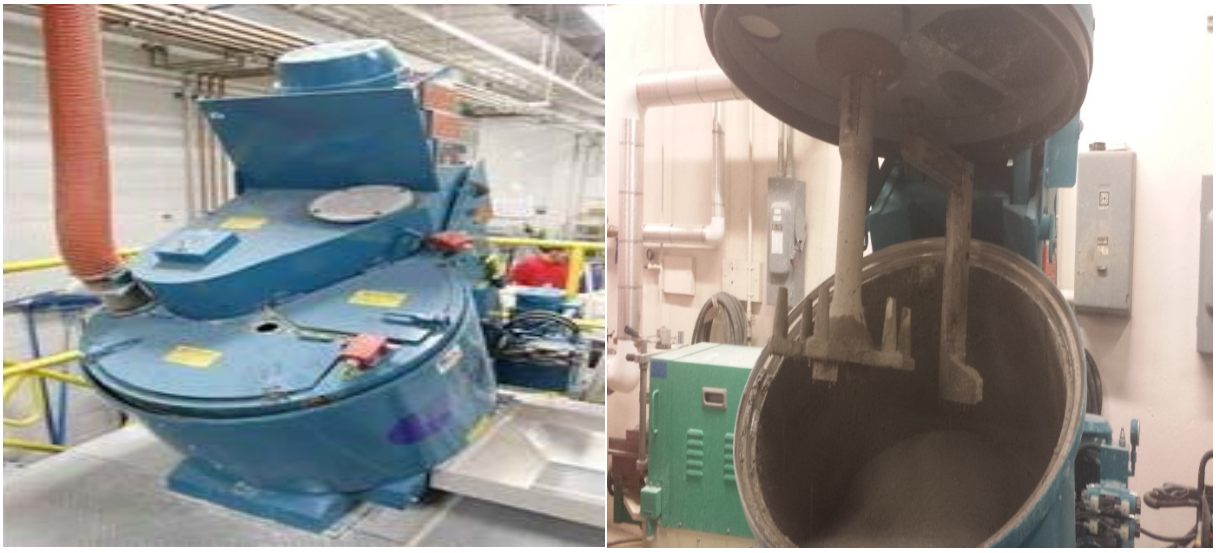

Figure 4. Eirich high-shear concrete mixer.

3.1.3 Mixing Procedure Cement Pastes Representing Pavement Concrete Mixtures

The mixing procedure was conducted according to ASTM C 305 using a Camframo BDC 2002 overhead stirrer mixer.

- All of the mixing water was placed in the bowl.
- The cement and ASCM was added in with the water and allowed to rest for 30 seconds.
- The mixer was started and mixed at a slow speed (140 +/- 5 rpm).
- The mixer was stopped for 15 seconds while the sides of the bowl were scrapped for material.
- The mixer was then mixed for 60 seconds at a medium speed (285 +/- 10 rpm).

3.1.4 Mixing Procedure for Pavement Concrete Mixtures

The mixing procedure was conducted according to ASTM C 192 using a drum mixer.

- The coarse aggregate and half of the mixing water was added to the drum and mixed.
- Then the mixer was started and the fine aggregate, remaining water with the admixtures, and cement and ASCM was added.
- The concrete was mixed for 3 minutes.
- Rested for 3 minutes while the drum opening was covered to prevent evaporation.
- Mixed for a final 2 minutes.
- The concrete was then removed and remixed by hand to prevent segregation.

3.2 Sampling and Curing

After the mixing was completed, the tests on fresh concrete were immediately conducted. These tests involved the measurement of the slump and air content of the concrete. For the structural concretes, rheological evaluation was also conducted. The tests on fresh concrete were conducted over a time interval of 75 minutes to monitor variations with time. After testing the fresh properties, the remaining concrete was mixed for 1 minute, and samples were produced. All samples were cast in three layers and vibrated for 20 seconds per layer. Specimens were covered and demolded after 24 hours, and they were further wet-cured at 23°C until the time of testing.

4 Experimental Methods

4.1 Tests on Fresh Cement Paste and Concrete

4.1.1 Foam Index Test

The foam index test was conducted on cement paste containing 25% replacement of perlite, pumice, and zeolite. This test attemps to determine the relative amount of AEA needed for concrete containing SCMs that affect air entrainment in concrete. The test used two AEA, referred to here as AEA 1 and AEA 2, on three different mixtures. The mixtures consisted of cement + AEA, SCM + AEA, and cement + 25% replacement of SCM + AEA.

There are many proposed versions of the foam index test, but currently there is no established standard for the test. Therefore, after an investigation of different methods, the following method was used. The test was run on each combination by mixing a 10 gram cement paste sample with a 0.45 water to cement ratio. An initial dilution of 1:10 of AEA was used for the test and was added drop by drop into a 250 mL wide-mouth Nalgene glass container with a lid. The mixture is shaken and agitated by hand for 30 seconds. The contents are observed for a stable foam that remains for 15 seconds (see Figure 5). If the stable foam was not achieved within 15 minutes, then the dilution was increased, Table 5 shows the dilution of AEA.

Figure 5. Examples of stable foams.

The foam index is the volume of diluted air entraining admixture solution added to the powder material, whereas the relative foam index is the ratio of air entraining admixture needed for a cementitious mixture containing ASCM with that required for just cement only, and is expressed as a percent of that required for just cement only. The following calculations were performed to determine the relative foam index of the ASCM-cement suspension.

$$\textit{Foam Index}_{cement} = N_{D\,cement} * 0.02 \quad (1)$$

$$\textit{Foam Index}_{ash} = N_{D\,ash} * 0.02 \quad (2)$$

$$\textit{Absolute Volume}_{cement} = N_{D\,cement} * 0.02 * C_{S\,cement} \quad (3)$$

$$\textit{Absolute Volume}_{ash} = N_{D\,ash} * 0.02 * C_{S\,ash} \quad (4)$$

$$\textit{Relative Foam Index} = [(\textit{Absolute Volume}_{ash}) / (\textit{Absolute Volume}_{cement})] * 100 \quad (5)$$

where N_d = total number of drops of air entraining admixture solution added to achieve stable foam, C_s = solution concentration of the air entraining admixture solution used, and Absolute Volume = volume of undiluted air entraining admixture solution added in the test.

Table 5. Dilution of air-entraining agents.

Dilution	AEA (mL)	Water (mL)
1:1	50	50
1:2	50	100
1:4	50	200
1:5	40	200
1:10	20	200

4.1.2 Mini Slump Flow Test for Cement Pastes Intended for Pavement Mixtures

The mini-slump flow test was conducted on cement paste containing 25% replacement of perlite, pumice, and zeolite. Each paste contained 375 grams of cement and 125 g of ASCM. The test was used to determine the compatibility of the paste with the AEA and HRWRA. A total of 1 mL of each AEA and 1 mL of HWRA were added to the paste and mixed according to ASTM C 1738 to determine if the cement paste was sufficiently flowable. The mini-slump was taken using a cone made of galvanized steel with a top diameter of 0.8 in., base diameter of 1.6 in., and a height of 1.4 in. The cement paste was placed in a single pour into the slump cone, and the diameter of the paste in two perpendicular directions was measured using a digital caliper. The average of these two diameters is reported as the mini-slump flow diameter.

4.1.3 Rheology of Cement Paste Intended for Structural Concrete Mixtures

The rheological properties of cement paste were characterized using the Anton Paar MCR 302 rheometer (Figure 6). A coaxial cylinders system was used having the following geometry: inner cylinder (R_i) = 13.385 mm, outer cylinder (R_o) = 14.562 mm, height (h) = 40.002 mm. Both the inner and outer cylinders had sandblasted surfaces to minimize slippage or the creation of a lubrication layer.

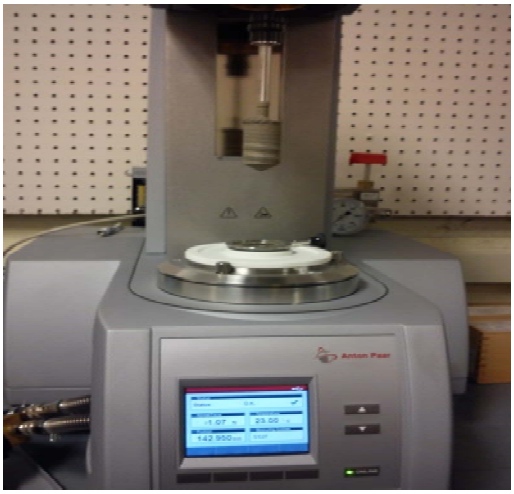

Figure 6. Anton Paar MCR 302 Rheometer used to determine the rheological properties of cement pastes.

The shear rate was decreased in 11 steps from 100 to 2 s^{-1}, maintaining each step for 5 s each, after a pre-shear period of 60 s at the maximum shear rate (100 s^{-1}) (Figure 7). At each step, equilibrium of the torque values was evaluated. If the step was in equilibrium the average of torque and rotational velocity was calculated during the last 4 s. If the torque was not in equilibrium, the point was discarded. The Reiner-Riwlin equation was applied on the obtained torque-rotational velocity data, resulting in yield stress and plastic viscosity values. However, the relationship between torque and rotational velocity deviates from the linear relationship at high SP dosages, requiring the application of a non-linear rheological model.

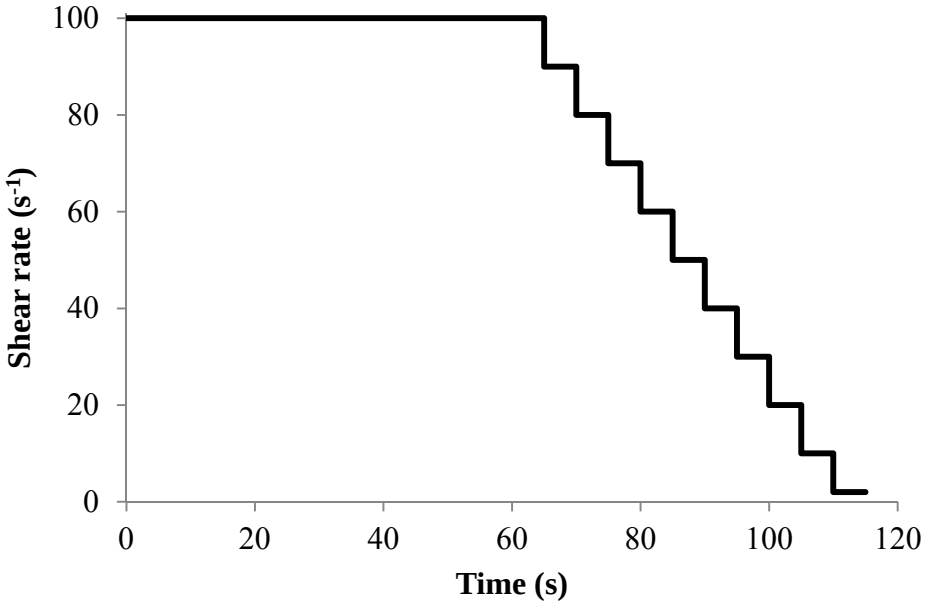

Figure 7. Testing procedure in Anton Paar MCR 302.

The modified Bingham model was used, which is described as follows (Eq.6):

$$\tau = \tau_0 + \mu \cdot \dot{\gamma} + c \cdot \dot{\gamma}^2 \qquad (6)$$

where τ_0 =yield stress [Pa], μ = linear term [Pa s], which can be interpreted as the viscosity of the material when it starts to flow, c = second order parameter [Pa s^2] is a parameter indicating shear thinning (c < 0), shear thickening (c > 0), or the Bingham model (c = 0). The determination of the yield stress based on the modified Bingham model is straightforward. The reported viscosities represent the inclination of the rheological curve at a shear rate of 50 s^{-1}.

4.1.4 Rheology of Concrete Intended for Structural Concrete Applications

The ConTec Viscometer 5 was used in this study to evaluate the rheological properties of concrete. It is a wide gap concentric cylinder rheometer with an inner radius of 100 mm and an outer radius of 145 mm. In order to prevent wall slip, both the inner and outer cylinders are provided with vertical ribs. The three dimensional complex flow at the bottom is avoided by the design of the inner cylinder, as it is divided into two parts and only measuring the torque at the upper part of the inner cylinder. The height of the upper part of the inner cylinder submerged in concrete is measured after each test. Figure 8 shows the ConTec Viscometer 5 rheometer.

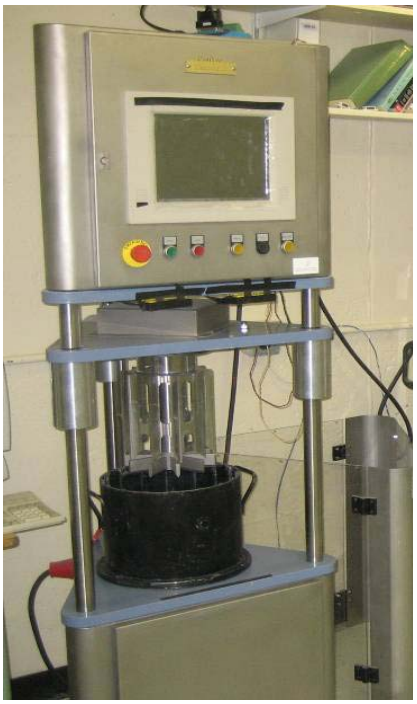

Figure 8. ConTec Viscometer 5.

Immediately after mixing, a fixed volume of concrete is poured into the rheometer bucket and brought to the rheometer. At 15, 45, and 75 minutes after first contact of water and cement, a preshear at a rotational velocity of 0.30 rps during 25 seconds was applied, followed by the stepwise decreasing rotational velocity profile from 0.30 to 0.025 rps, in 10 steps of 5 s each. Only the last 4 s of each rotational velocity step re considered during the analysis.

After plotting the measured rotational velocity and torque values versus time, a visual check of the data can verify if segregation occurred during the experiment and if all the rotational velocity steps are in equilibrium. When the torque measurement during a constant rotational velocity step was not in equilibrium, it was not considered in the analysis. For all mixtures, the torque – rotational velocity diagram was linear and thus, the Bingham model was applicable. The dynamic yield stress and plastic viscosity were calculated assuming the Bingham fluid model (Eq. 7) in which τ is the shear stress, $\dot{\gamma}$ is the shear rate, τ_0 is the dynamic yield stress, and μ_p is the plastic viscosity. When plug flow occurred, a plug flow correction was performed [24].

$$\tau = \tau_0 + \mu_p \cdot \dot{\gamma} \tag{7}$$

4.1.5 Slump and Air Content in Fresh Concrete

The consistency and air content of fresh concrete were monitored over time according to ASTM C 143 and ASTM C 231, respectively.

4.2 Tests on Hardened Cement Paste and Concrete

4.2.1 Compressive strength

For each testing age, three 4×8 in. cylindrical specimens were used for determining the compressive strength according to ASTM C39. The concrete cylinder end was grinded at all test ages for the structural concrete, whereas the ends of the cylinder were capped with rubber pads for the pavement mixtures.

4.2.2 Modulus of Elasticity (conducted on structural concrete mixtures)

Two 4×8 in. cylindrical specimens were tested at the age of 56 days to determine the static modulus of elasticity according to ASTM C469. The test setup included the specially designed axial deformation measuring device shown in Figure 9. The two parallel rings are both rigidly attached to the cylinder with a 51-mm (2-in.) gage length between attachment points. The upper ring holds three linear variable displacement transducers (LVDTs) whose ends bear on the lower ring. Thus, the axial deformation of the cylinder can be measured. The load and the output from the three LVDTs were digitally recorded through the test.

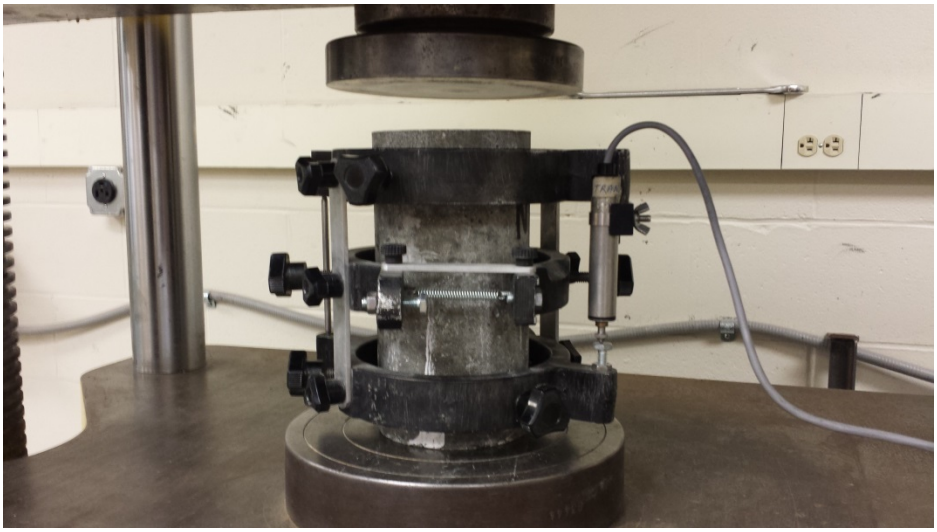

Figure 9. Test set-up of modulus of elasticity test.

The loading cycles were repeated three times for each sample. The vertical strain of the specimen corresponding to each stress level was measured using the LVDT system. The results were then used for determining the modulus of elasticity based on the following equation:

$$E = \frac{S_2 - S_1}{\varepsilon_2 - 0.000050} \quad (8)$$

where E = Chord modulus of elasticity (psi), S_2 = stress corresponding to 40% of the ultimate load capacity, S_1 = stress corresponding to a longitudinal strain of 0.000050, and ε_2 = longitudinal strain caused by the stress S_2.

4.2.3 Splitting Tensile Strength (conducted on structural concrete mixtures)

Three 4×8 in. cylindrical specimens were tested at the age of 56 days to determine the splitting tensile strength according to ASTM C496 and the mean values were reported. The splitting tensile test setup is shown in Figure 10. Compressive loads (P) are applied on the top and bottom of the specimens where two

strips of plywood are placed to apply the load along a vertical plane through the specimens. The load at failure is recorded as the peak load, and the tensile strength is calculated using the following equation:

$$F_t = \frac{2P}{\pi DL} \quad (9)$$

where F_t = splitting tensile strength (psi), P = ultimate load at failure (lb), D = sample diameter (in.), and L = sample length (in.).

Figure 10. Splitting tensile strength setup.

4.2.4 Flexural Strength (Modulus of Rupture) (conducted on structural concrete mixtures)

The flexural strength, also known as modulus of rupture, was measured on 6×6×21 in. beams in accordance with ASTM C78. Two specimens were tested for each concrete mixture at the age of 56 days and the mean values were reported as flexural strength of the concrete. A four-point bending setup was used for testing the flexural strength. Figure 11 depicts a schematic view of the test setup used for loading the beams. Two rigid supports were located approximately 1.5 in. away from each side of the specimen. The load was applied on the concrete beam and the failure load (P) was recorded. The flexural strength is then calculated using the following equation:

$$R = \frac{Pl}{bh^2} \quad (10)$$

where R = modulus of rupture (psi), P = the ultimate load (lb), l = span length equal to 18 in., b = average beam width at fracture (in.), and h = average beam height at fracture (in.).

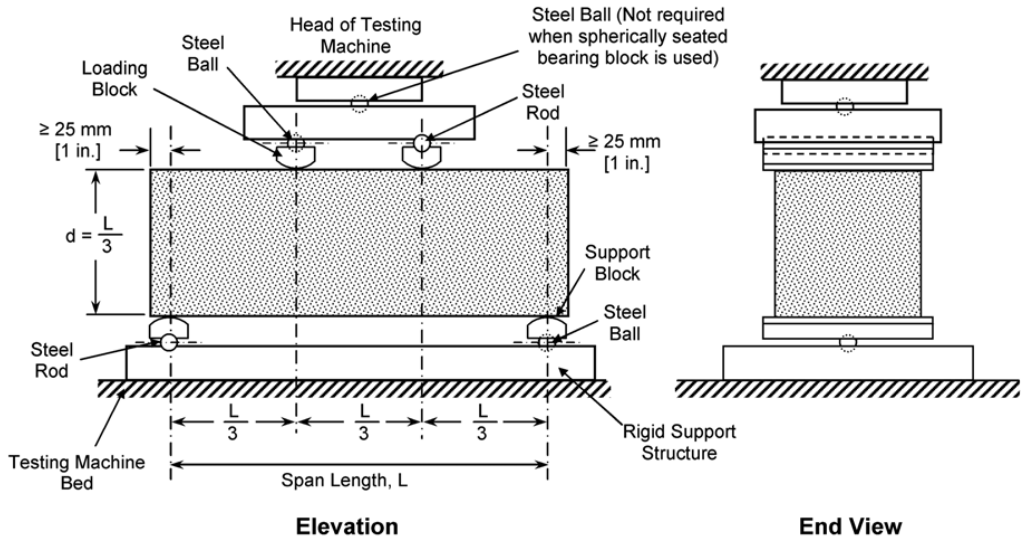

Figure 11. Schematic overview of flexural strength tests (ASTM C78).

Figure 12. Flexural strength test.

4.2.5 Air-Void System Analysis (conducted on pavement mixtures)

Hardened Cement Paste - The hardened paste air void analysis was conducted to determine the ability to maintain air voids in the paste specimens. A constant dosage rate of AEA, 1 mL, was used for all ASCMs, the ASCMs were compared for analysis on how they interact with the 1 mL of AEAs in 750 grams of cement and 250 grams of ASCM.

After the paste was measured for slump (see section 4.1.5), the paste was cast in a 2x4" cylinder in one continuous pour. The specimen was then placed in a fog room to cure for 7 days. Once cured, the cylinder was cut into thirds with a wet saw. To measure the air voids on each surface, the target surface was

grinded and polished into a smooth surface. The flat surfaces were colored white a fine-tipped black marker and the voids were filled with (white) barium sulfate. The colored surfaces were scanned and then analyzed in an image editor to determine the percentage of voids.

Hardened Concrete - The hardened air-void analysis investigated the air void system at a microscopic level. By analyzing the air voids in hardened concrete this provided a more comprehensive understanding of the durability of the concrete for freeze-thaw resistance.

From the original pour, each mixture was cast in a polystyrene box for use in the hardened air void analysis. The specimens were wet cut from the cast into a 1" slice from the middle. The surface of the samples was prepared according to ASTM C 457. A thinned lacquer (20% lacquer/80% acetone) was applied to the surface to strengthen the paste and reinforce the voids. After twenty four hours, the samples were grinded down using an 80-grit, 100-grit, 180-grit, and 260-grit paper while applying lacquer in between increasing grit size. Once the specimen was finished, the surface was viewed under a microscope at 20x and 50x to ensure the surface is completely polished. The sample was soaked in acetone to remove the thinned lacquer. Then surface was colored with a fine-tipped black marker and the voids were filled with (white) barium sulfate. The specimens were analyzed using a RapidAir 457 air void analyzer.

4.2.6 Surface Electrical Resistivity Test

Resistivity is a material property that quantifies the degree to which an object prevents the passage of an electrical current. While the solid material in concrete has a relatively high resistivity, the pores are partially to fully saturate with a concentrated alkaline solution that has a relatively low resistivity. Thus, electrical current flows primarily through the pore solution, giving an indirect measure of the quality of the microstructure.

The Resipod resistivity meter, with uniform electrode spacing of 1.5 in., was used to measure the surface resistivity of cylindrical concrete specimens. The Resipod is a resistivity meter operating on the principle of the Wenner probe. The Wenner probe consists of four equally spaced, co-linear electrodes that are placed in contact with a concrete cylinder specimen. An alternating current is applied to the outermost electrodes and the voltage between the middle two electrodes is used to determine the resistance as shown in Figure 13.

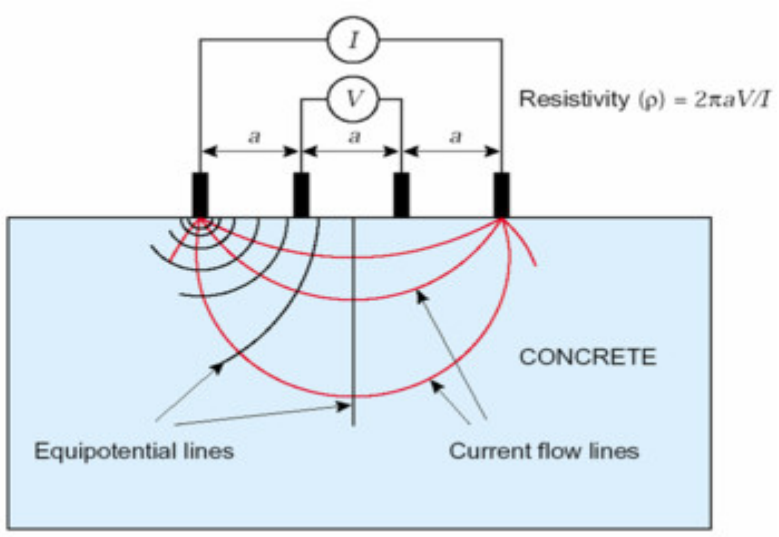

Figure 13. A schematic overview of the surface resistivity test.

The current is carried by the ions available in the pore solution. The sample resistivity is calculated from the resistance, the distance between the electrodes and the dimensions of the cylinder using the following equation:

$$\rho = 2\pi aV/I \tag{11}$$

where: ρ = surface resistivity (kΩcm), a = electrode spacing (1.5 in.), V = potential difference (V), I = applied electric current.

This method is also applicable on field measurements for predicting the likelihood of corrosion due to chloride diffusion as well as estimating the corrosion rate once depassivation of the steel has taken place. Considering the reduced time and effort required for conducting the surface resistivity test, many agencies are moving towards this method to replace alternative time consuming methods such as the rapid chloride ion permeability test (RCPT), chloride ponding, etc [25]. The empirical criteria suggested by the manufacturer are presented in Table 6 [26]. These criteria can be used to determine the likelihood of corrosion on flat surfaces in the field.

Table 6. Correlation between the surface resistivity and likelihood of corrosion.

Concrete Resistivity	Likelihood of Corrosion
≥100 kΩcm	Negligible risk of corrosion
=50-100 kΩcm	Low risk of corrosion
=10-50 kΩcm	Moderate risk of corrosion
≤10 kΩcm	High risk of corrosion

In this study three 4×8 in. cylindrical specimens were used for determining the surface resistivity. The same specimens were used for tests at different ages to monitor the variations in electrical resistivity with time. Specimens were kept in lime saturated water up to the test time. Before starting the test, specimens were thoroughly washed to ensure performing measurements on a clean surface. Table 7 presents the criteria to predict the corrosion rate based on the surface resistivity on flat surfaces while referring to depassivated steel [26].

Table 7. Correlation between the surface resistivity and rate of corrosion.

Concrete Resistivity	Estimated corrosion rate
>20 kΩcm	Low corrosion rate
10-20 kΩcm	Low to moderate corrosion rate
5-10 kΩcm	High corrosion rate
<5 kΩcm	Very high corrosion rate

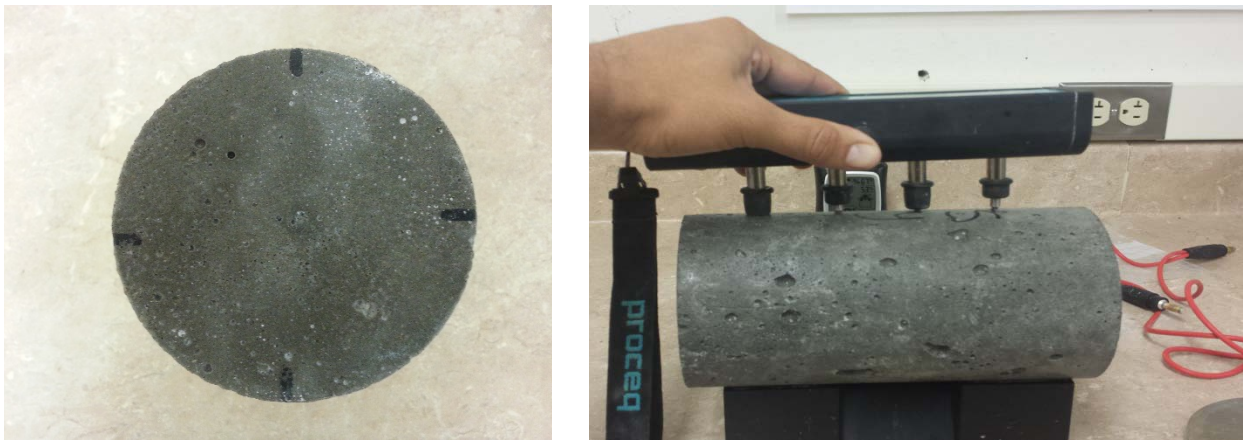

Figure 14. Surface resistivity measurement.

A good connection between the electrodes and the concrete surface is the most important factor affecting the reliability of measurements. Therefore, the test surfaces were kept wet during the test period to maintain a good connection. For each specimen, four separate readings were taken around the circumference of the cylinder at 90-degrees Increments (0º, 90º, 180º, and 270º). Measurements were repeated several times at each angle to find the most reliable reading. Figure 14 shows the procedure of surface resistivity test.

4.2.7 Bulk Electrical Conductivity

The bulk electrical conductivity of the specimens was measured using the Resipod test setup. The same samples used for the surface resistivity test were used for measuring the bulk conductivity according to ASTM C1760. In order to conduct this test, it is required to put pieces of wet foam on top and bottom of the specimen, between the concrete surface and the metal plates of the test setup. The foam pieces ensure

proper electrical contact to the cylinder. However, depending on the moisture condition, these foam pieces will also have some electrical resistivity that should be taken into account to determine the true value of the sample's bulk resistivity. Figure 15 shows the three steps required for bulk resistivity measurements.

First, the resistivity of the upper foam should be determined (R_{upper}). Then, the bottom foam should be placed between the plates, with the specimen on the top plate to simulate the effect of the weight of the specimen on foam thickness and porosity. The resistivity of the bottom foam should be recorded (R_{lower}). Finally, the bulk resistivity of the sample with foam at top and bottom should be measured ($R_{measured}$). Using the following equation, the net bulk resistivity of the sample can be calculated:

$$R_{cylinder} = R_{measured} - R_{upper} - R_{lower} \quad (12)$$

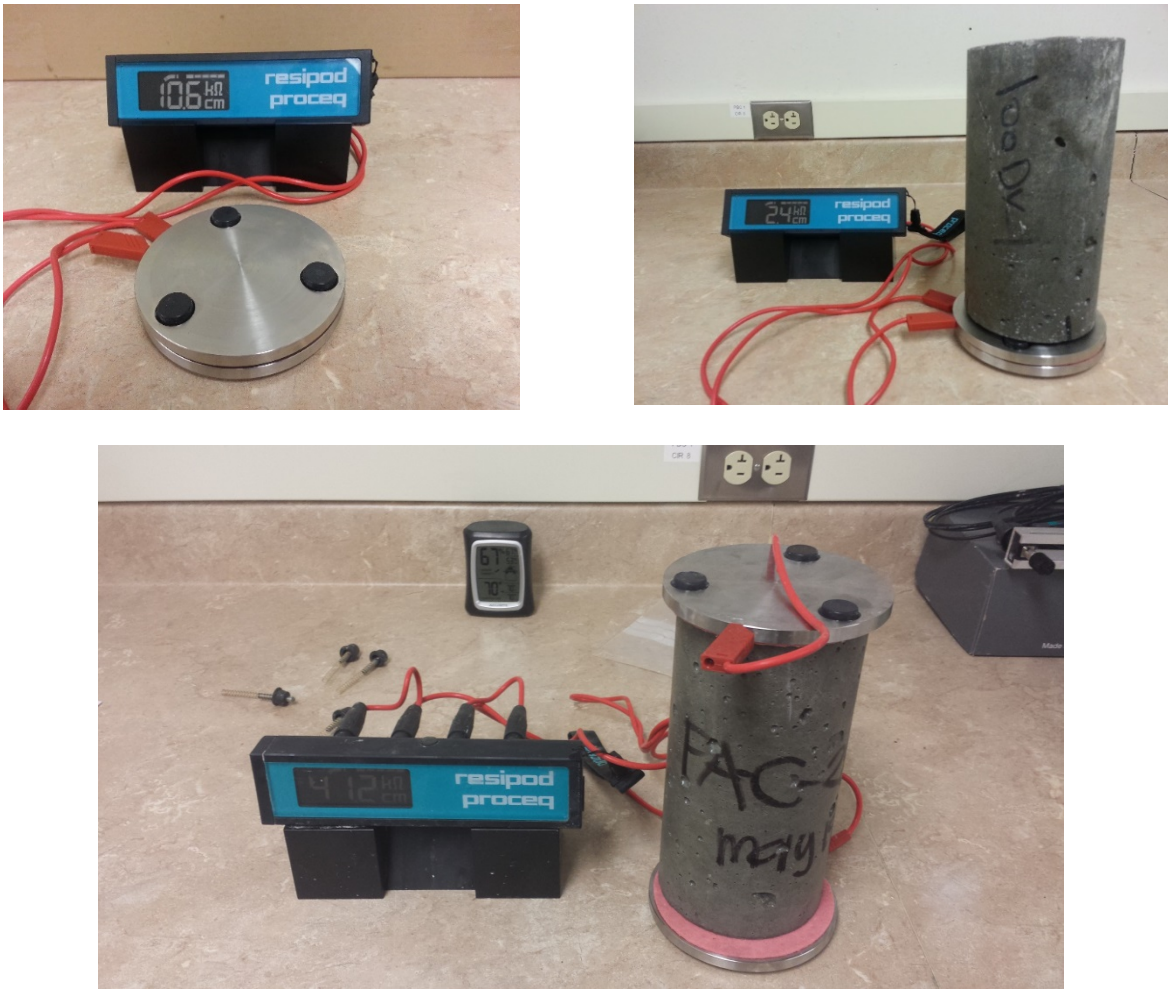

Figure 15. Measuring bulk electrical resistivity. Top foam (top left), lower foam (top right), and specimen resistivity (bottom).

4.2.8 Permeable Void Volume and Absorption

The ASTM C642 method measures the volume of permeable voids of a concrete sample as a percentage of the volume. This method determines the water absorption after immersion in water at room temperature and after immersion in boiling water for five hours. The high temperature affects both the

viscosity and the mobility of the water molecules which may enable a greater displacement of water within the pore system of the hardened concrete [27]. Two samples were used for determining the permeable void volume. These samples were half cylinders measuring 4 in. in diameter and 4 in. in height. These samples were obtained by cutting a 4×8 in. cylinder into two pieces. This way, each specimen had finished, formed, and cut surfaces exposed to water penetration. Samples were dried in an oven at a temperature of 220 ± 40 °F up to a constant mass (measures the decrease in mass of hardened concrete which has been dried until 2 weighing, taken 24 h apart, result in a change in mass of less than 1%). The oven dried mass of the samples was measured after cooling down to room temperature (A). The specimens were then immersed in water in room temperature up to a time when the specimen was completely saturated and the saturated surface dried (SSD) mass of the specimen was constant. After registering this weight (B), the specimens were immersed in boiling water for five hours, followed by a 14 hours period of rest to cool down to room temperature. The SSD weight after boiling was measured in this step (C). Finally, the submerged weight of specimens was determined (D). The following equations were used for measuring the absorption, density, and permeable void volume of the specimens:

$$\text{Bulk dry density } (g_1) = [A/(C-D)]\times\rho\times 100 \quad (13)$$

$$\text{Apparent density } (g_2) = [A/(A-D)]\times\rho\times 100 \quad (14)$$

$$\text{Permeable void volume } (\%) = (g_2-g_1)/g_2 \times 100 \quad (15)$$

Where ρ is the density of water equal to 1 g/cm^3.

Absorption of the concrete samples is measured for both the saturated and boiled conditions according to the ASTM C642 test method. The following equations are used for calculating the absorption of the samples after immersion and after boiling:

$$\text{Absorption after immersion} = [(B-A)/A] \times 100 \quad (16)$$

$$\text{Absorption after immersion and boiling} = [(C-A)/A] \times 100 \quad (17)$$

Where “A” is the oven dry weight, “B” is the SSD weight after immersion, and “C” is the SSD weight after immersion and boiling.

5 Results and Discussion

5.1 Foam Index of Cement Pastes

Table 8 presents the results of the foam index test. It appears that AEA1 would be more effective in achieving a stable air void system than AEA2 (compare the absolute volumes of the suspensions prepared with AEA1 vs those prepared with AEA2), however regardless of the AEA used, incorporation of an ASCM increased AEA demand. For AEA1, AEA demand increased by 50% for all of the cement-ASCM suspensions compared to the plain cement suspensions. Whereas when AEA 2 was employed, AEA demand increased by 150% when 25% of the cement (by mass) was replaced with perlite or zeolite, and it increased by 200% when pumice was used as a cement replacement material. The relative foam index ratio for the three ASCMs suggests that the pumice acts as a sink and that a cementitious composite prepared with pumice would require a substantially higher AEA dosage than composites that are prepared using perlite or zeolite, especially when AEA1 is used. However, comparison of the relative foam indices of the suspensions containing cement and an ASCM appears to indicate otherwise. Interestingly, the relative foam index ratios of the cement + perlite, cement+pumice, and cement+zeolite suspensions are fairly equal for a given AEA.

Table 8. Relative foam index ratio required per SCM.

	AEA 1					AEA 2				
Suspension	N_d	C_s	Foam Index	Absolute Volume	Relative Foam Index Ratio	N_d	C_s	Foam Index	Absolute Volume	Relative Foam Index Ratio
Cement	2	0.1	0.4	0.04	N/A	7	0.1	1.4	0.14	N/A
Cement + Perlite	3	0.1	0.6	0.06	**1.5**	5	0.1	1	0.1	**2.5**
Perlite	13	0.5	2.6	1.3	32.5	4	0.1	0.8	0.08	2
Cement + Pumice	3	0.1	0.6	0.06	**1.5**	6	0.1	1.2	0.12	**3**
Pumice	20	0.5	4	2	50	13	0.1	2.6	0.26	6.5
Cement + Zeolite	3	0.1	0.6	0.06	**1.5**	5	0.1	1	0.1	**2.5**
Zeolite	19	0.1	3.8	0.38	9.5	9	0.1	1.8	0.18	4.5

where N_d = total number of drops of air entraining admixture solution added to achieve stable foam, C_s = solution concentration of the air entraining admixture solution used, Foam Index = volume of diluted air entraining admixture solution added in the test, Absolute Volume = volume of undiluted air entraining admixture solution added in the test and, Relative Foam Index = ratio of air entraining admixture needed for cementitious mixture containing SCM with that required for just cement only.

5.2 Mini Slump for Cement Paste

Similar fluidity levels were seen in the pastes regardless of the AEA that was used, and the cement-zeolite paste displayed the lowest slump (see Table 9). This is consistent with the rheological testing results seen in TxDOT project 0-6717 for these materials. Mini-slump flow has been shown to be inversely related to yield stress, thus the higher the yield stress of a material, the lower its mini-slump would be. In TxDOT project 0-6717, higher yield stress values were observed in pastes containing the zeolite vs the pumice or

perlite. The low slump flow behavior of the cement-zeolite paste is attributed to the high surface area and highly porous structure of the zeolite.

Table 9. Comparison of mini-slump flow diameter for cement-ASCM pastes for a constant AEA and HRWR dosage

	AEA1 Diameter (in)	AEA2 Diameter (in)
Pumice	5.983	6.422
Pearlite	6.855	7.350
Zeolite	1.519	1.630

5.3 Saturation Point of HRWRA in Presence of SCMs

In order to determine the saturation point, five different cement paste mixtures were considered. The mix design for 1 liter of cement paste presented in Table 10. For the plain cement mixture, the water-to-cement ratio was set at 0.35 (by mass) and the SP/C (by weight of active admixture ingredient) was increased per 0.1%. The SCMs were incorporated replacing 20% of the cement by volume. The volume of water, and the incremental amounts of SP added were identical for all mixtures. It should, however, be noted that the w/cm and the SP/C vary due to the volumetric replacement of cement by the SCM.

Table 10. Mixture Proportioning of Cement Pastes (in g/l)

Materials	Cement	Cement-FA	Cement-PL	Cement-PM	Cement-ZL
Cement	1494	1192	1192	1192	1192
Water	523	523	523	523	523
Superplasticizer increments	1.5	1.5	1.5	1.5	1.5
FA	-	258	-	-	-
PL	-	-	226	-	-
PM	-	-	-	234	-
ZL	-	-	-	-	226

An example of the obtained torque versus rotational velocity data in the Anton Paar MCR 302 for perlite is presented in Figure 16.

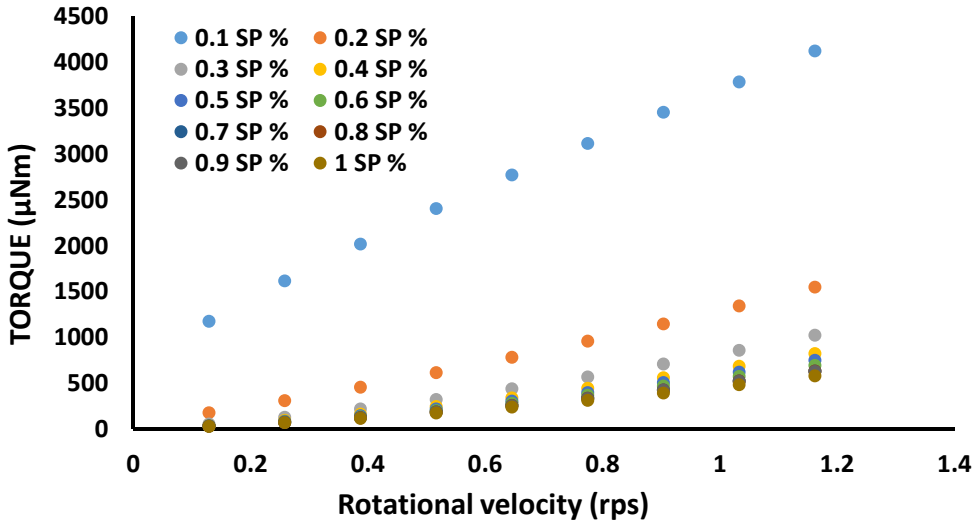

Figure 16. Torque as a function of the rotational velocity for perlite at different dosages of SP.

As expected, the results indicate that the yield stress and the viscosity decrease with increasing dosage of superplasticizer. The zeolite showed higher yield stress and viscosity values compared to the other SCMs. The saturation dosage was determined as the dosage of SP, relative to the amount of cement, beyond which the yield stress and viscosity values did not substantially vary (Figure 17 and Figure 18). For plain cement paste and pastes with 20% fly ash or 20% perlite (by vol.), the same saturation dosage (0.3 % by mass of binder) was obtained. The admixture saturation dosage for pumice and zeolite was higher. Table 11 presents the SP saturation dosage for all the paste.

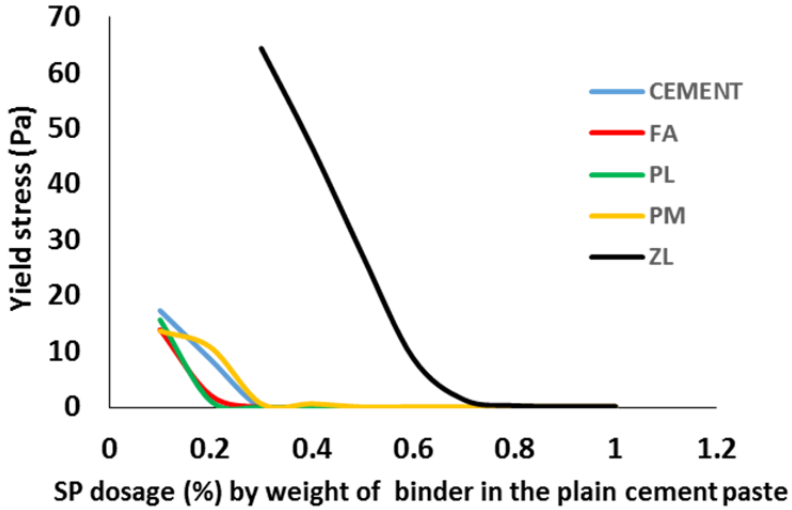

Figure 17. Yield stress of the pastes versus SP addition.

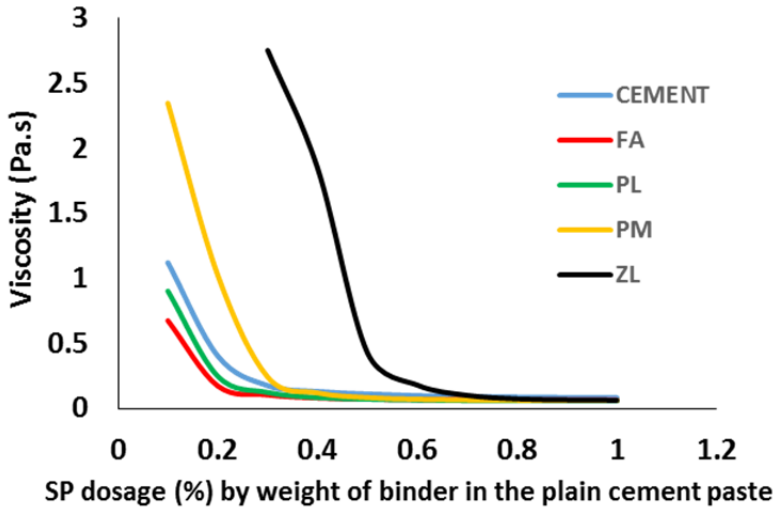

Figure 18. Viscosity of the pastes versus SP addition.

Table 11. SP saturation dosage (% by weight of binder)

	Cement	Cement-FA	Cement-PL	Cement-PM	Cement-ZL
SP dosage	0.3	0.3	0.3	0.5	0.7

5.4 Workability Retention of Cement Pastes for Infrastructure

The rheological properties are followed with time to investigate the workability retention. The main objective of this task is to understand the workability loss of the cement pastes with time, as a function of the use of SCM and at different temperatures. Furthermore, additional replacement rates of cement by SCM were investigated, dependent on the outcome of the workability retention.

The cement paste mix designs are identical to the ones represented in Table 10. The HRWRA dosage is chosen at 2/3rd of the saturation dosage to avoid sedimentation of the sample during the measurement period. For each SCM, an additional replacement rate was investigated for workability retention. Due to the high demand of HRWRA and the elevated rheological properties, the chosen replacement was 10 % by volume of cement for pumice and zeolite. Seen the good performance of the fly ash and perlite, additional tests were performed at 30% replacement by volume for these materials.

The investigation on the workability retention is performed with the Anton Paar MCR 302, in the same configuration as the one used for the saturation point determination. The same testing procedure to determine the rheological properties of the paste is repeated at 10, 30, 60 and 90 min after the addition of the water. The tests are performed at 10, 23 and 35°C to investigate the influence of temperature on workability retention.

Figure 19 to Figure 24 show the evolution of the yield stress and viscosity with time at 10, 23 and 35 °C respectively. As can be seen in the figures, the mixture with pumice shows a larger increase of yield stress and plastic viscosity with time, compared to the mixtures with perlite or fly ash, or the plain cement

mixtures, regardless of temperature. The results also show that the incorporation of perlite and fly ash reduces the increase of yield stress and viscosity with time compared to the plain cement mixture.

As shown in Figure 20, zeolite showed the lowest workability retention, even at the lower replacement rate. Also pumice had poor workability retention, regardless the replacement rate. The results indicate that the incorporation of perlite and fly ash resulted in excellent workability retention, even at high replacement rate. However, compared to fly ash the addition of perlite was found more effective in reducing the yield stress at lower (10 °C) and higher temperature (35 °C).

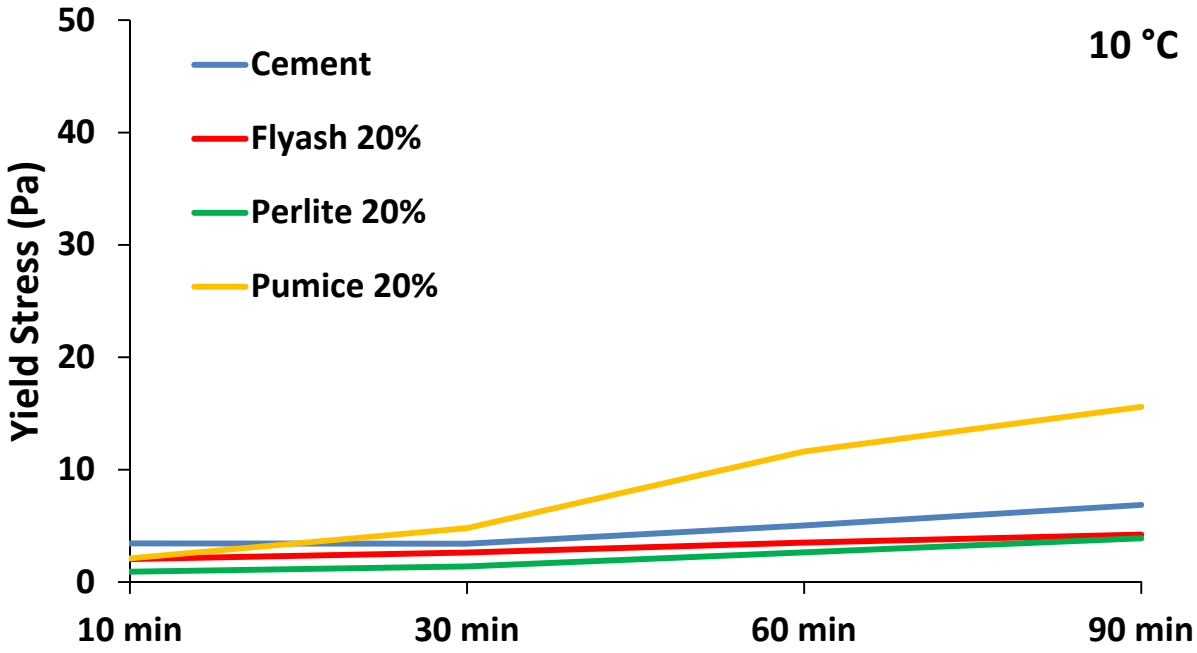

Figure 19. Yield stress vs time of cement paste with different SCMs at 10 °C.

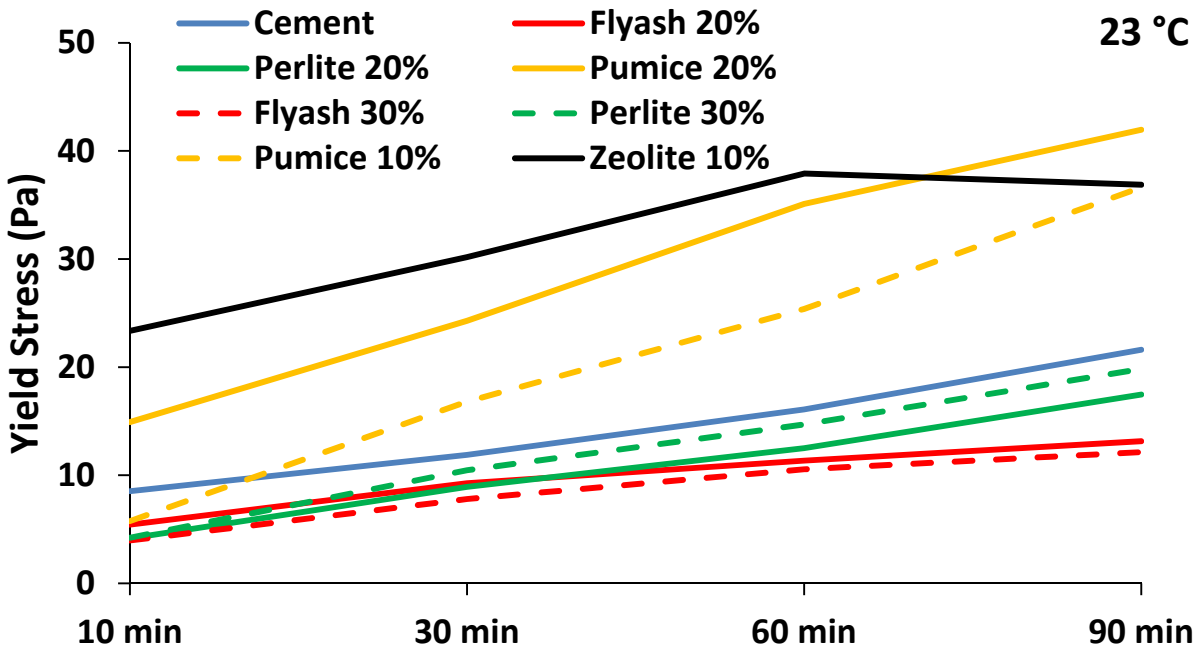

Figure 20. Yield stress vs time of cement paste with different SCMs at 23 °C.

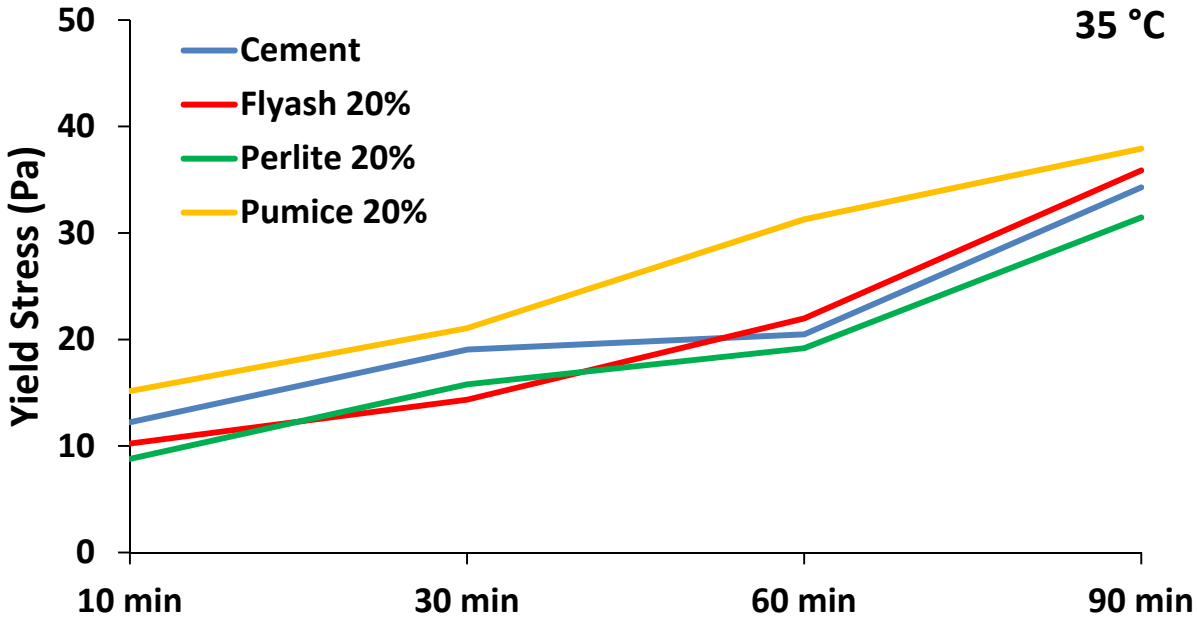

Figure 21. Yield stress vs time of cement paste with different SCMs at 35 °C.

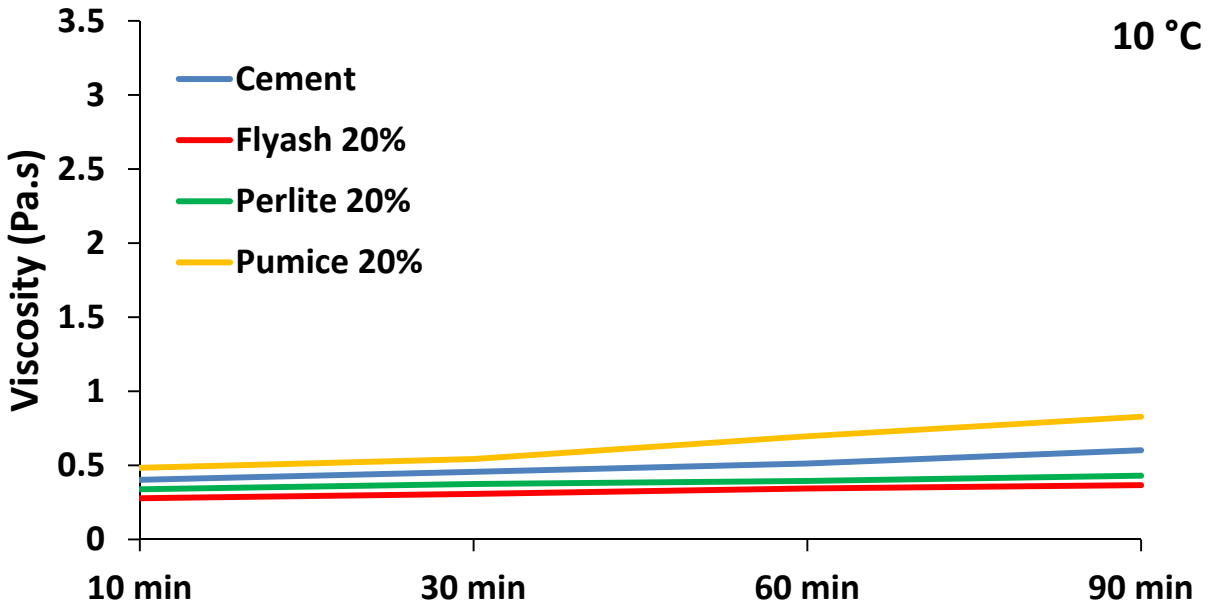

Figure 22. Viscosity vs time of cement paste with different SCMs at 10 °C.

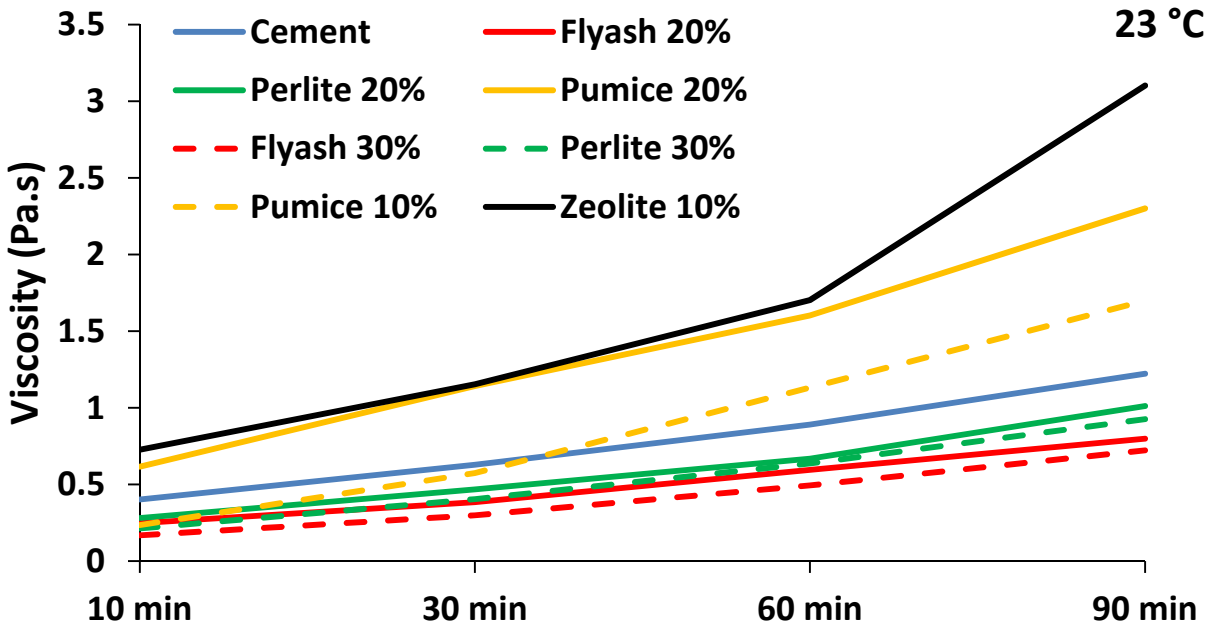

Figure 23. Viscosity vs time of cement paste with different SCMs at 23 °C.

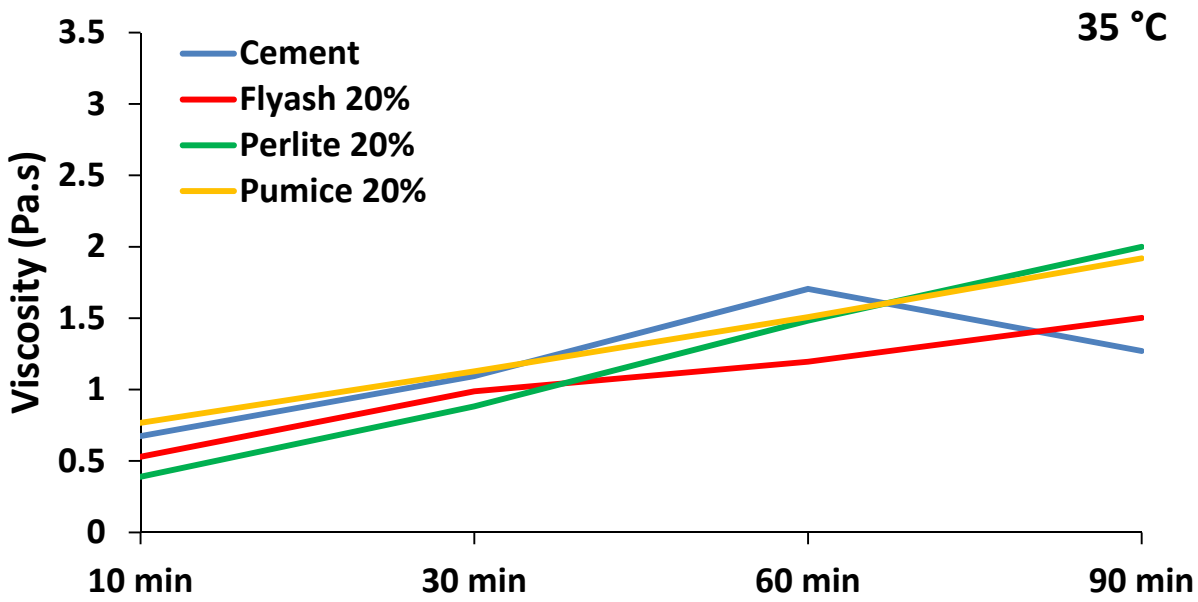

Figure 24. Viscosity vs time of cement paste with different SCMs at 35 °C.

Figure 25 to Figure 28 show the effect of temperature on yield stress and viscosity evolution with time as a function of temperature for the mixtures with fly ash and perlite, respectively. As can be seen, both yield stress and viscosity increase faster with increasing temperature, which is in accordance with results from literature. For the mixtures with plain cement, fly ash and perlite, no substantial difference in workability retention is noticed at each temperature.

In summary, the replacement of cement by pumice (at 20% by vol) reduces the workability retention of the cement paste, while the use of fly ash or perlite has no significantly positive nor negative effect on the workability retention, compared to the plain cement mixture. The workability retention at different temperatures is in agreement with literature, independent of the material used.

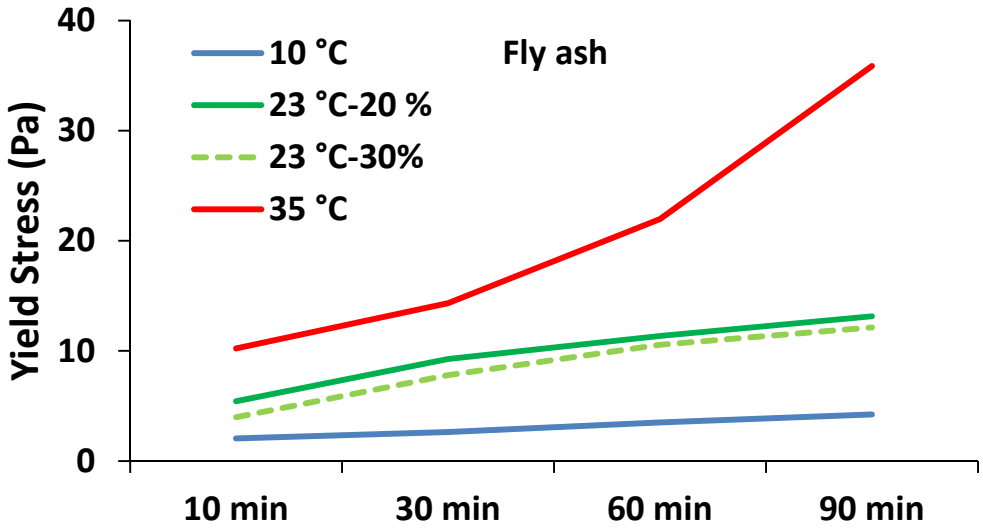

Figure 25. Yield stress vs time of cement paste with fly ash at different temperatures.

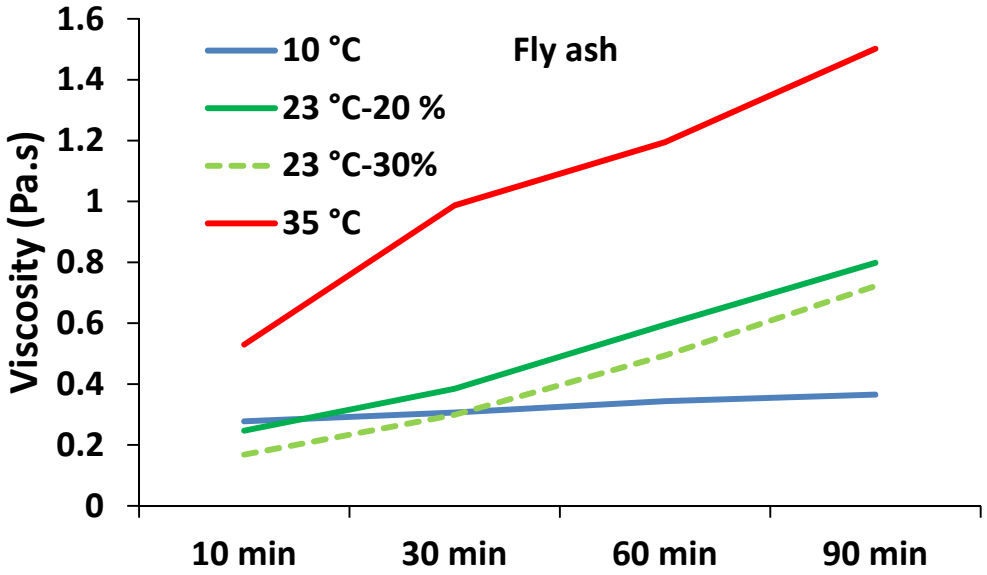

Figure 26. Viscosity vs time of cement paste with fly ash at different temperatures.

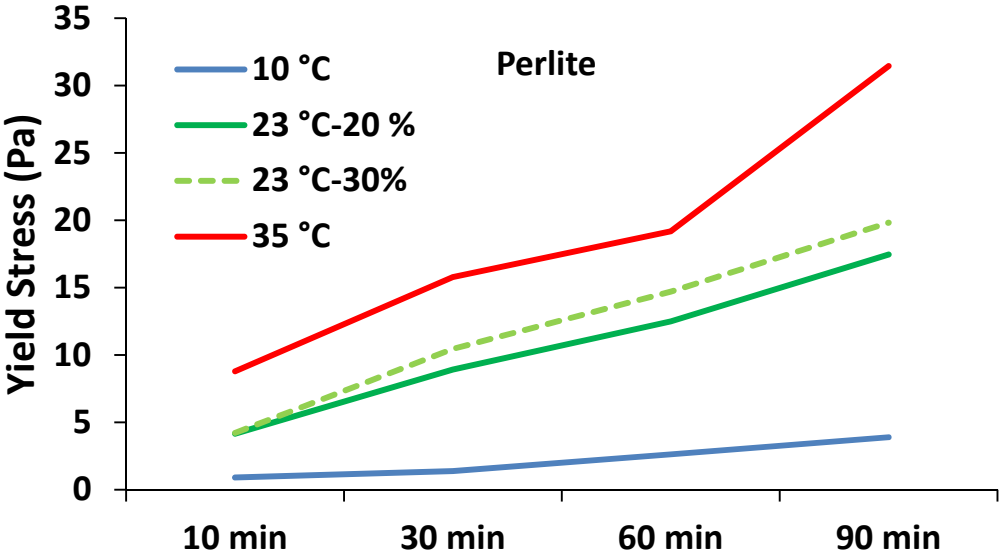

Figure 27. Yield stress vs time of cement paste with perlite at different temperatures.

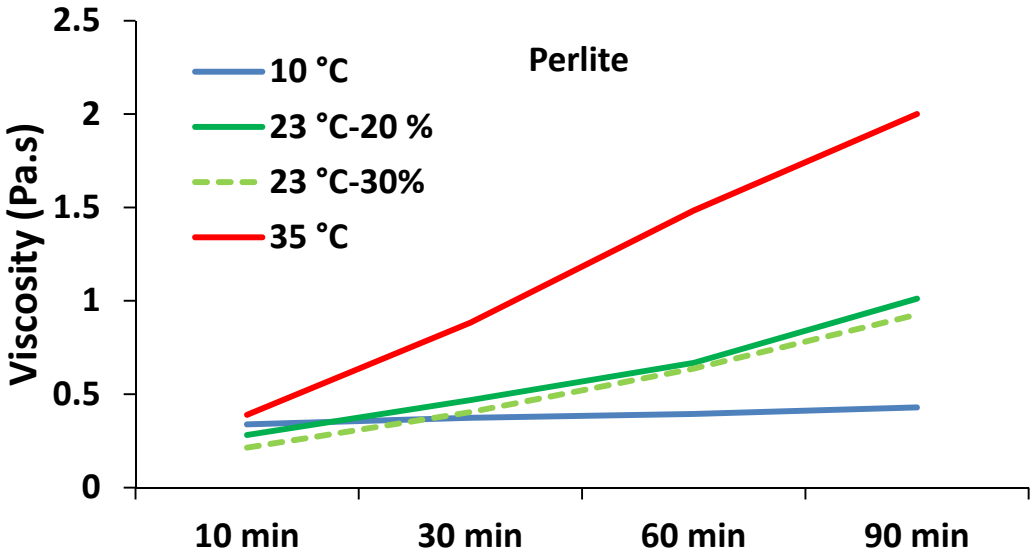

Figure 28. Viscosity vs time of cement paste with perlite at different temperatures.

5.5 Fresh Properties of Concrete for Pavement

The analysis for the air void content was determined through an iterative process in order to achieve the target slump and air content as per recommendation by ACI 211 and TxDOT, respectively. The initial objective was to achieve a workable slump of 2 in. (± 0.5 in.) using the WRA, and then aim to get the target air content of 5.5% ± 0.5% by adding AEA 1. The air content was determined using a pressure air meter conforming to ASTM C231.

Table 12 presents the properties of the concrete batch used for all tests and the dosages of HRWR and AEA. The admixture demand for zeolite superseded both the pumice and perlite significantly. The zeolite has an extremely porous structure which was likely a large factor in the high demand of both the HRWR and AEA. The pumice and perlite have a similar structure, with the perlite having slightly higher water content. Therefore, the perlite had a lower demand for both admixtures.

Table 12. Admixture demand (AEA 1 and HRWRA) to reach desired slump and fresh concrete air content.

25% SCM	HRWRA (fl oz./lb cement)	AEA 1 (fl oz./lb cement)	Slump (in)	Air Content (%)
Zeolite	14.00	3.00	2	5.5
Pumice	0.56	0.51	2.25	5
Perlite	0.41	0.35	2.5	5

5.6 Fresh Properties of Concrete for Structural Concrete

In general, two series of concrete mixtures were considered in which the two different types of AEA were used. The proportions of all the mixtures are presented in Table 13. The mixtures were designed to resist severe corrosion: class C2 according to the ACI Building Code. The water to cementitious materials

(w/cm) ratio was kept constant at 0.4 by weight of cement. The plain cement mixture, with slump of 8.5 in (at 15min), served as a reference for each series. The amount of SP was adjusted in order to achieve the same slump value. The evolution of the fresh state properties including slump, yield stress and viscosity was recorded through the time.

Table 13. Mix design of concrete mixtures (in kg/m^3)

Materials	REF	Concrete-FA	Concrete - PL	Concrete - PM	Concrete - ZL
Cement	388	291	291	330	349
Coarse aggregate	940	933	926	933	934
Fine aggregate	770	764	758	764	765
SCM	-	97	97	58	39
Water	155	155	155	155	155
SP (gr/m^3)	1.22	0.48	0.4	1	1.61
AEA Type 1 (gr/m^3)	0.26	0.26	0.26	0.26	0.26
AEA Type 2(gr/ m^3)	0.18	0.18	0.18	0.18	0.18

5.6.1 Air Content

The air-void system created by using air-entraining agents (AEA) in concrete is influenced by the concrete materials and construction practices [28]. It has been reported that air content will increase as cement alkali levels increase and decrease as cement fineness increases significantly [29]. In this study, the air content in fresh concrete was measured by pressure method at 15 and 70 min. Before each measurement the concrete was mixed for 30 seconds. The effect of two different types of AEA, including AEA 1 and AEA 2 on the air void system of the mixtures has been studied. All mixtures were designed to reach 7-8% air content (at 15 min). Figure 29 shows the air content of concrete mixtures with AEA 1. As can be seen, the air content of all concrete mixtures decreases with time. A dramatic change was observed for the mixture containing fly ash. The negative effect of fly ash on concrete air entrainment has been widely reported [30-32]. The mixture containing pumice has the most stable air-void system among all tested SCMs after 70 minutes, which is in contrast with the results in section 4.2.5. The reason for this difference is still unknown. Figure 30 presents the air content of the mixtures with AEA 2. The FA-mixture shows the lowest air content after 70 min while the mixtures containing perlite and pumice have more stable air. Also the results indicated that AEA 2 has more stable air regardless of the type of SCMs used in the mixture.

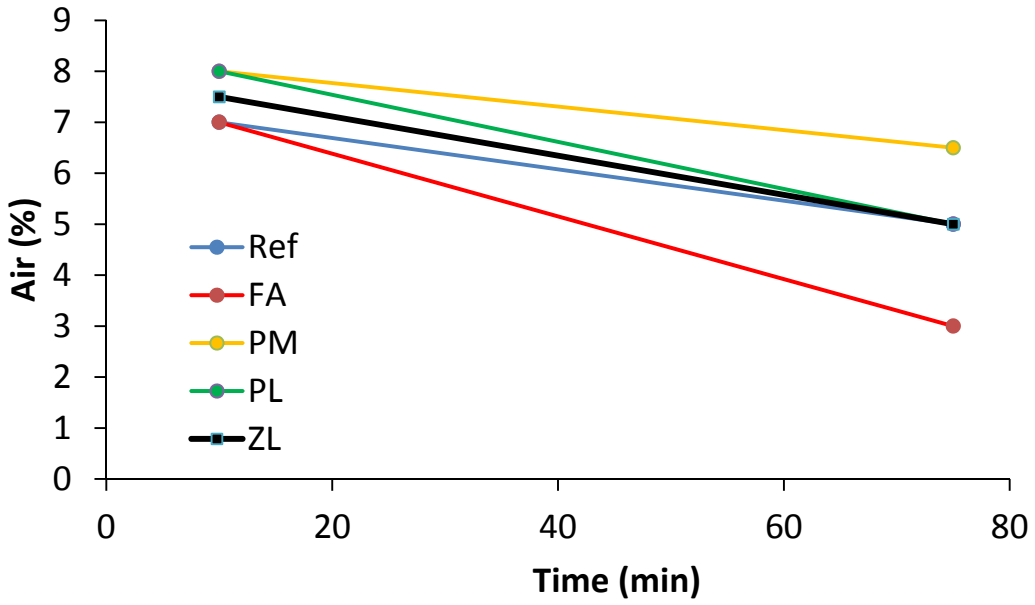

Figure 29. The air content of AEA 1-mixes at 15 and 70 min.

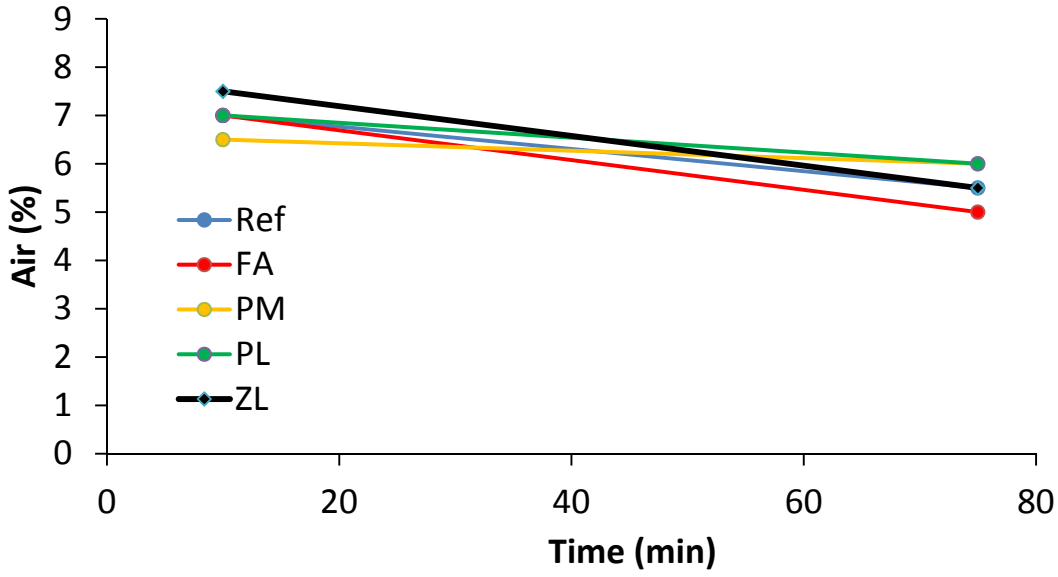

Figure 30. The air content of AEA 2-mixes at 15 and 70 min.

5.6.2 Concrete Consistency: Slump Test

The slump test was performed at 15 min, 40 and 70 minutes. Before each measurement the concrete was mixed for 30 seconds. The amount of SP was adjusted for all mixtures to ensure an initial slump of 8.5-9 in. The results for slump retention for both series of mixtures are presented in Figure 31 and Figure 32. As shown, the replacement of cement by perlite and fly ash enhances the workability retention. The high

slump loss can be observed for zeolite and pumice mixes. The slump evolution with time on concrete is in agreement with the workability retention on the cement pastes, discussed above.

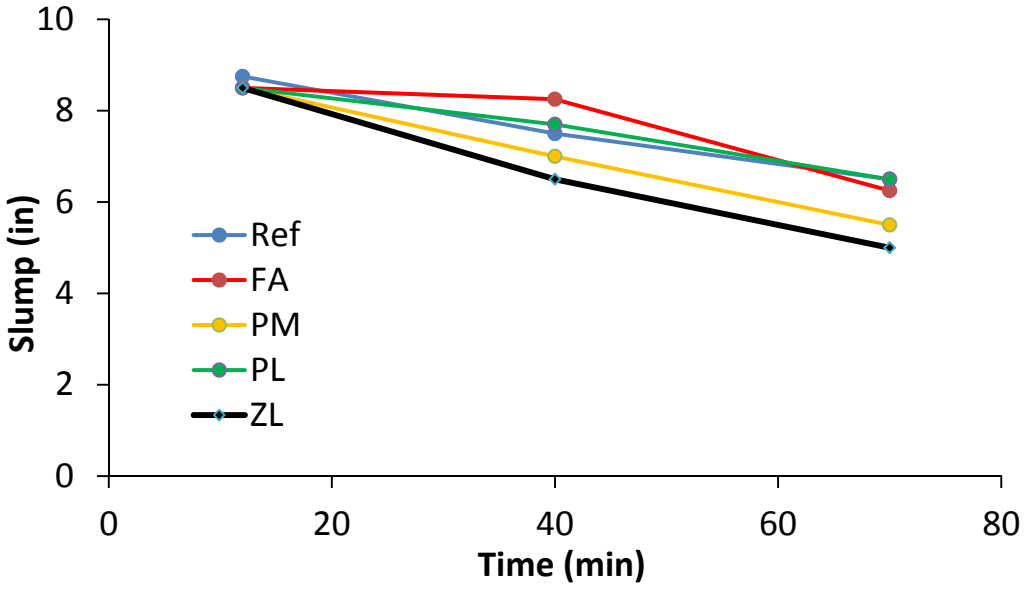

Figure 31. Slump retention of AEA 1-mixtures at 15, 40 and 70 min.

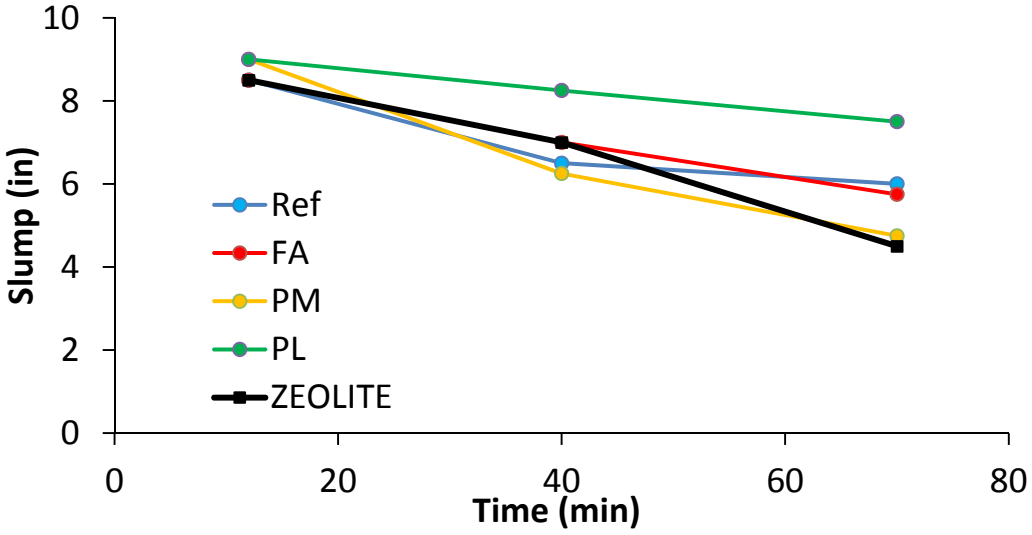

Figure 32. Slump retention of AEA 2-mixtures at 15, 40 and 70 min.

5.6.3 Rheological Properties

Figure 33 to Figure 36 show the evolution of the yield stress and viscosity with time at 15, 45 and 75 min. The results show that the mixtures with pumice and zeolite have a larger increase of yield stress and plastic viscosity with time, compared to the mixtures with perlite or fly ash, or the plain cement mixtures. It was observed that the inclusion of perlite and fly ash reduces the yield stress and viscosity with time

compared to the plain cement mixture. The achieved rheological results were in good agreement with workability retention of the cement pastes and the values obtained by the slump test.

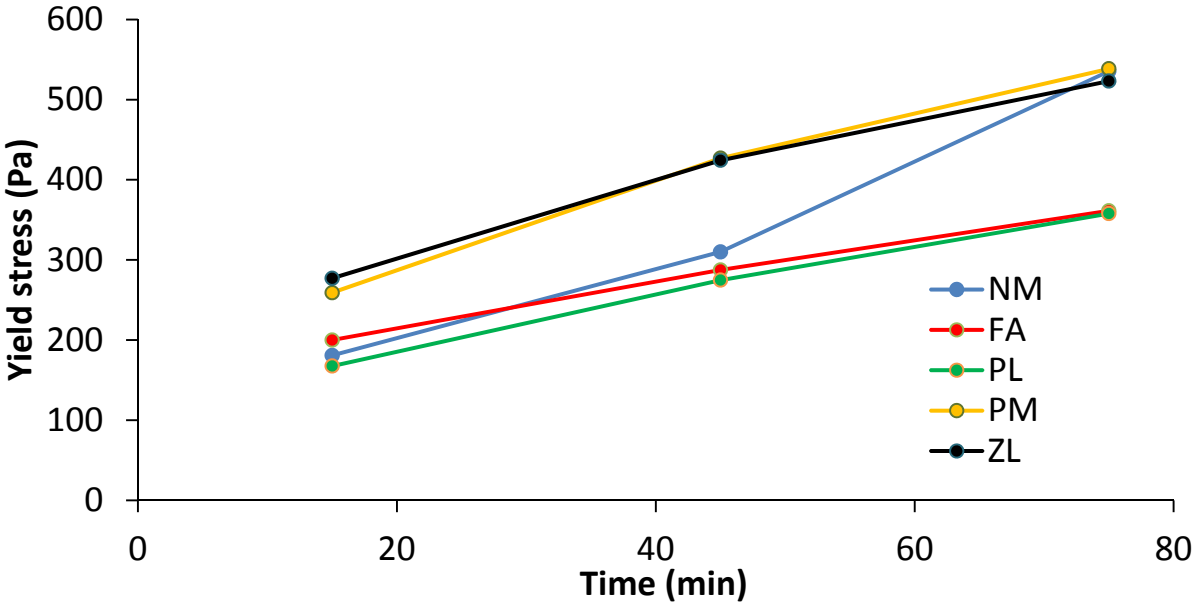

Figure 33. Yield Stress of AEA 1-mixtures at 15, 45 and 70 min (NM is reference plain cement mixture).

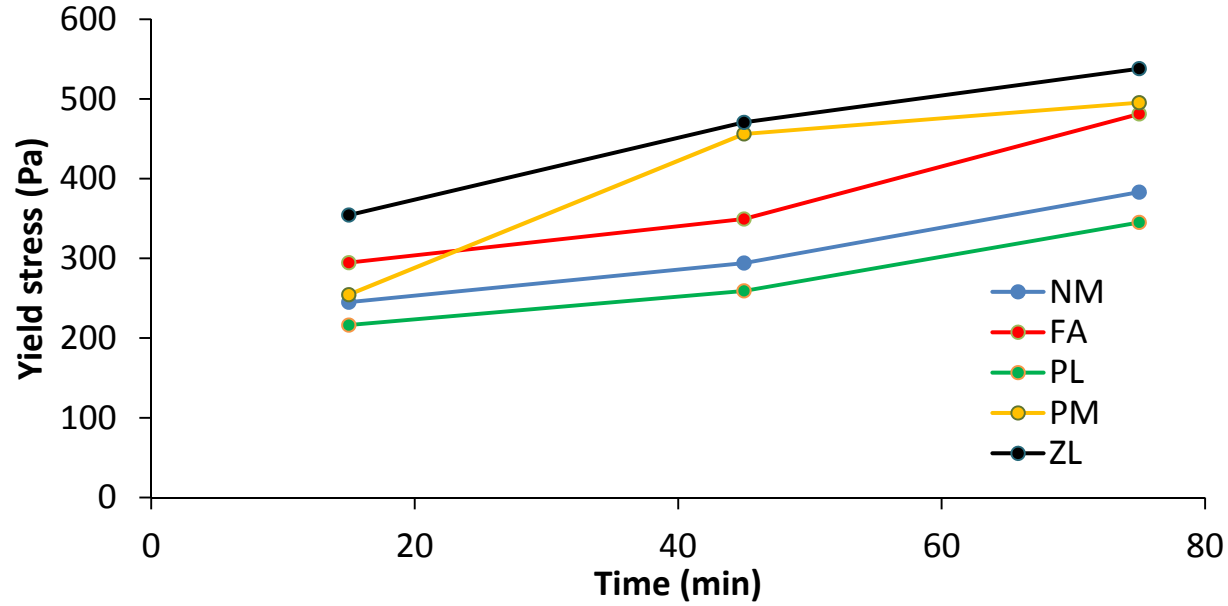

Figure 34. Yield Stress of AEA 2-mixtures at 15, 45 and 70 min (NM is reference plain cement mixture).

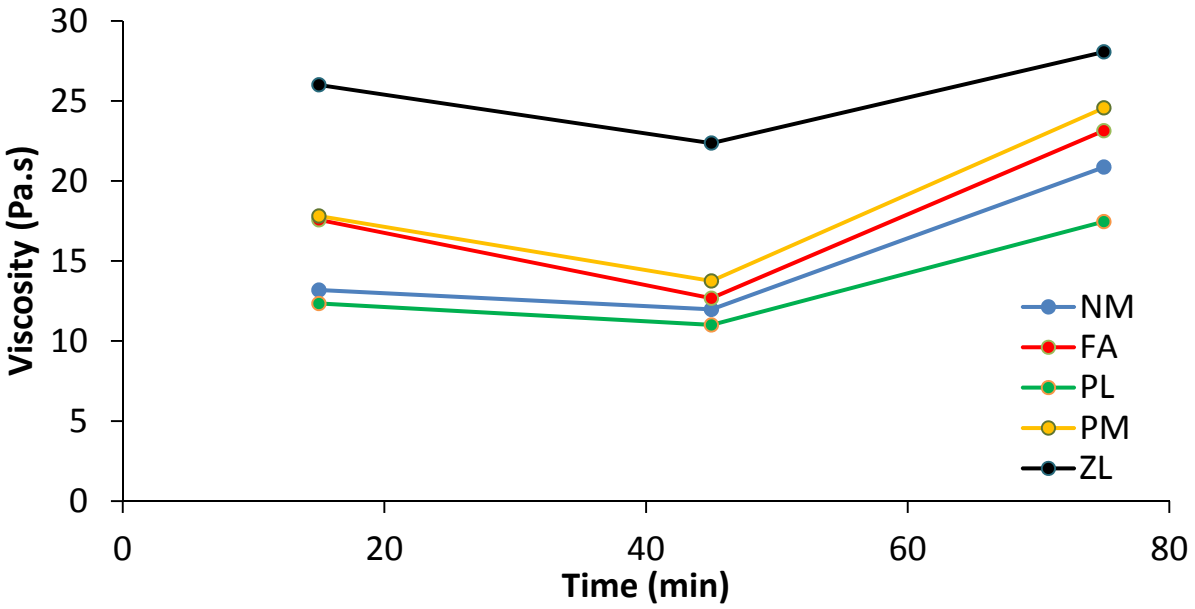

Figure 35. Viscosity of AEA 1-mixtures at 15, 45 and 70 min (NM is reference plain cement mixture).

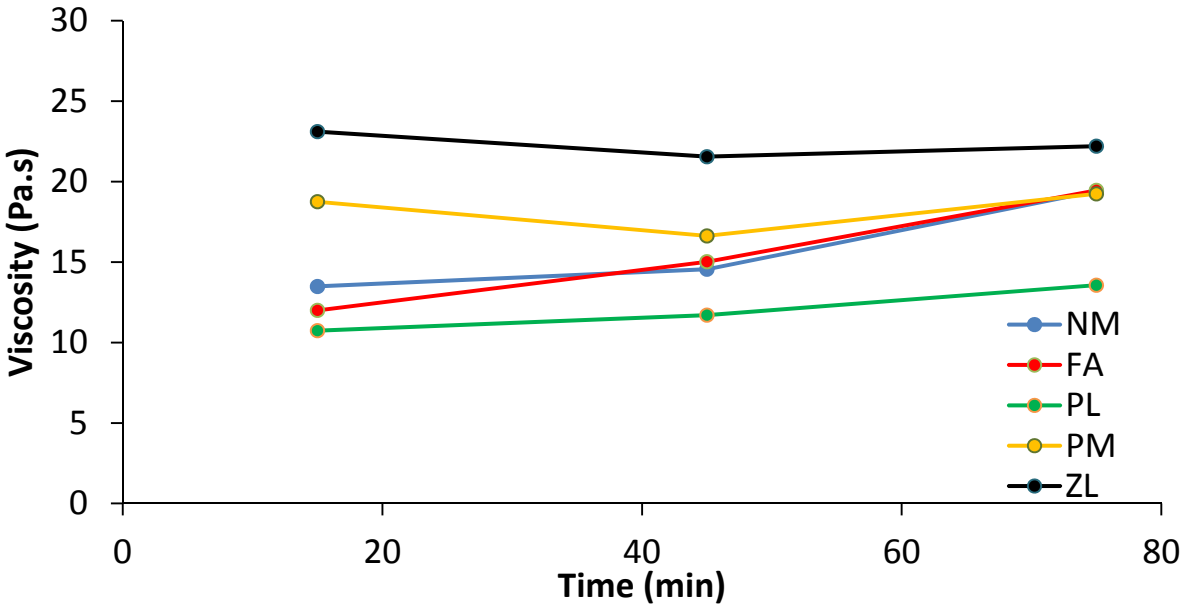

Figure 36. Viscosity of AEA 2-mixtures at 15, 45 and 70 min (NM is reference plain cement mixture).

5.7 Heat of Hydration Measurements on Cement Paste

The heat of hydration of cement pastes with 20% replacement (by vol.) of cement with SCM was determined by means of calorimetric measurements. The reference paste (100% cement) had a w/cm = 0.45 and a SP dosage = 0.5 % by volume. The water and SP dosage was kept constant for all other pastes, prepared with the different SCMs. In order to stabilize the temperature of water, it was kept in the

calorimeter for two hours prior to mixing. Afterwards the water and SP was added to the cementitious materials and the pastes were manually stirred with a spatula for 3 min. The test duration was 48 h.

From the results obtained through isothermal calorimetry, presented in Figure 37 and Figure 38, the zeolite accelerated the hydration reaction significantly and released almost the same cumulative heat compared to the plain cement paste, while pumice accelerated the reaction slightly during the first 12 hours of the test. On the other hand, the maximum heat flow reached by perlite was the lowest for all tests and the total accumulated heat was also the lowest. Fly ash delayed the hydration reaction slightly and its cumulative heat released was similar to pumice at the end of the test.

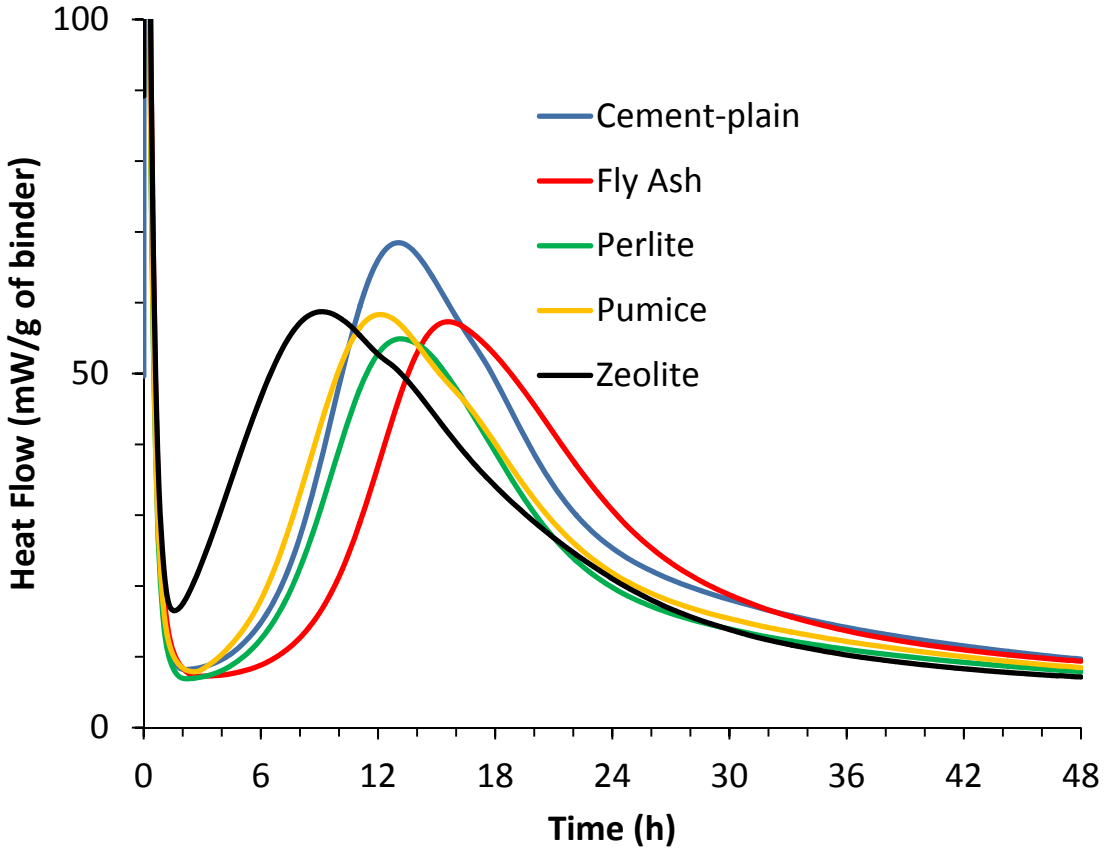

Figure 37. Heat flow in isothermal calorimeter of cement pastes produced with different SCMs.

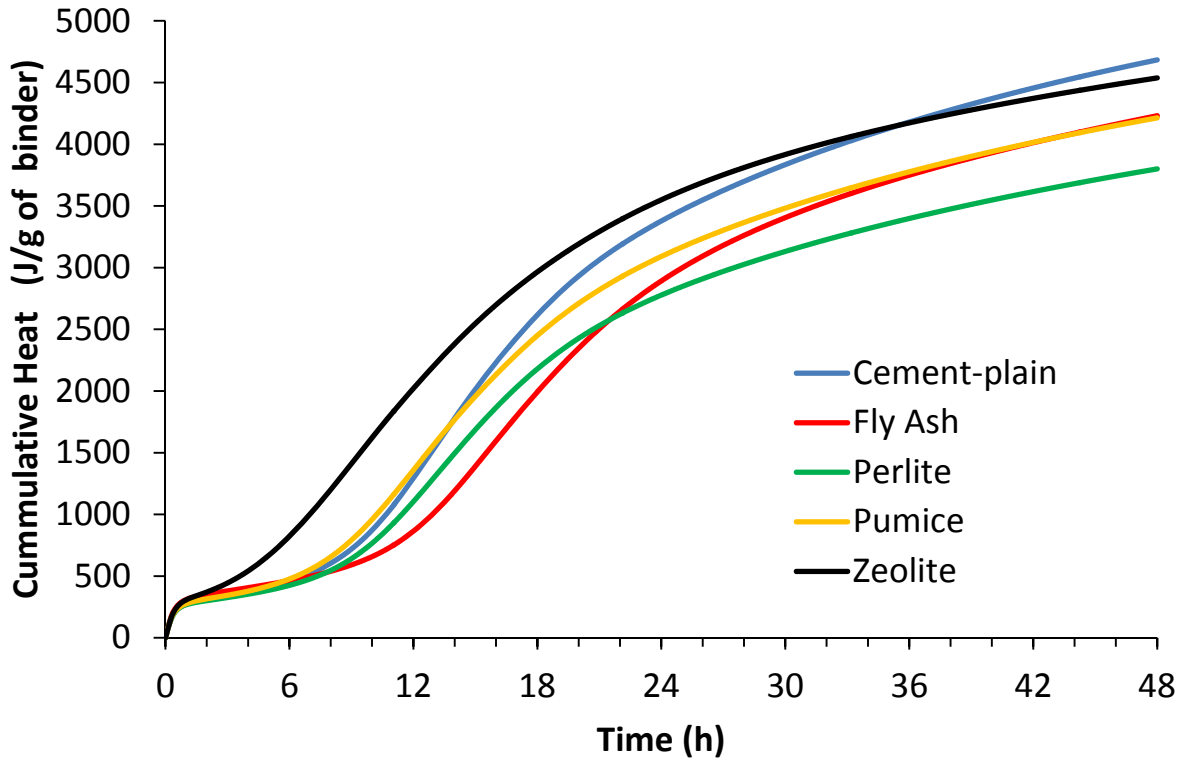

Figure 38. Cumulative heat released during hydration of cement pastes produced with different SCMs.

5.8 Compressive Strength Evolution of Hardened Concrete for Pavement

Compressive strength measurements were conducted at 1, 14, 28, and 56 days according to ASTM C 39 (Figure 39). The results indicate that the zeolite produced stronger concrete at day 28 by more than 40%. But all three mixes satisfied the minimum specified concrete strength of 3000 psi according to ACI 318 for use in construction as a pavement concrete. As the percent of voids in concrete increases, the compressive strength decreases. This is consistent with the data collected by Project 0-6717 which each contained 2% air. The SCMs with the air entrainment followed the same strength gain pattern consistent without air entrainment [23].

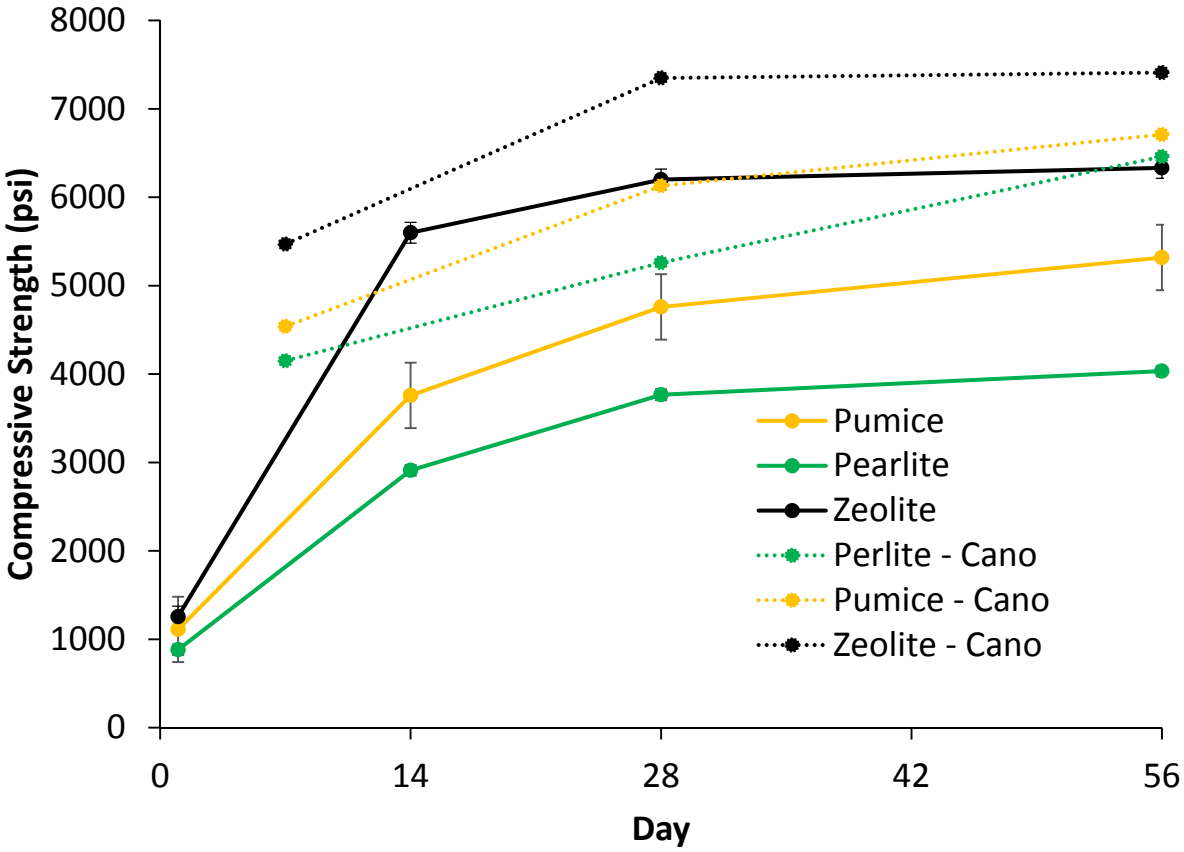

Figure 39. Compressive strength gain of concrete for pavement. The dashed lines represent the results from [23], using the same SCMs without the AEA.

5.9 Mechanical Properties of Hardened Concrete for Structural Applications

5.9.1 Compressive Strength

The average values of compressive strength at 1, 7, 28 and 56 days are shown in Figure 40, for the AEA 1 specimens. Compared to the reference mixture, the results indicated that the incorporation of perlite, pumice, zeolite and fly ash led to a decrease of 1-day concrete compressive strength by 31%, 27%, 21%, and 12% respectively. However, it can be seen that the addition of ZL significantly increased the early-age compressive strength beyond 1 day. The higher compressive strength is due to faster pozzolanic reactivity of zeolite particles, in the presence of $Ca(OH)_2$, making the microstructure denser. In addition, the incorporation of ZL particles can accelerate the hydration process due to the large and highly reactive surface area [33-35]. These results are consistent with the results of hydration calorimetry analysis. A slight increase in 28 and 56 days compressive strengths of specimens containing pumice and fly ash was observed compared to the reference mixture. In general, the addition of perlite resulted in a decrease of compressive strength, even at later age.

Figure 41 shows the average values of compressive strength at the different ages for concrete made with AEA 2. As can be seen, the ZL-mixture showed the highest compressive strength at all the ages, except at

one day. Similar to the AEA 1 specimen results, the PL-mixture showed the lowest compressive strength. However, the addition of Pumice and FA showed almost the same strength values as the reference mixture.

Also for the AEA 2 concrete, the PL and PM mixtures had lower compressive strengths compared to the same mixture in AEA 1. As mentioned before, the air void system was less stable in mixtures with AEA 1. According to Figure 30, the more stable air void system can be observed for perlite and pumice mix which can be indicative of a lower compressive strength.

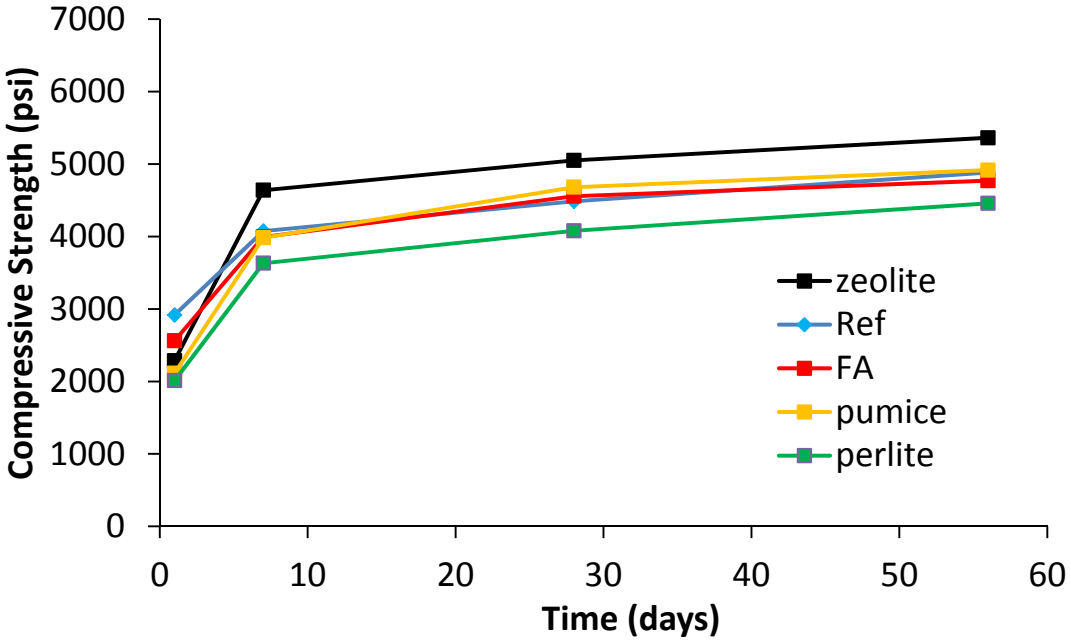

Figure 40. Compressive strength of AEA 1 specimens versus time.

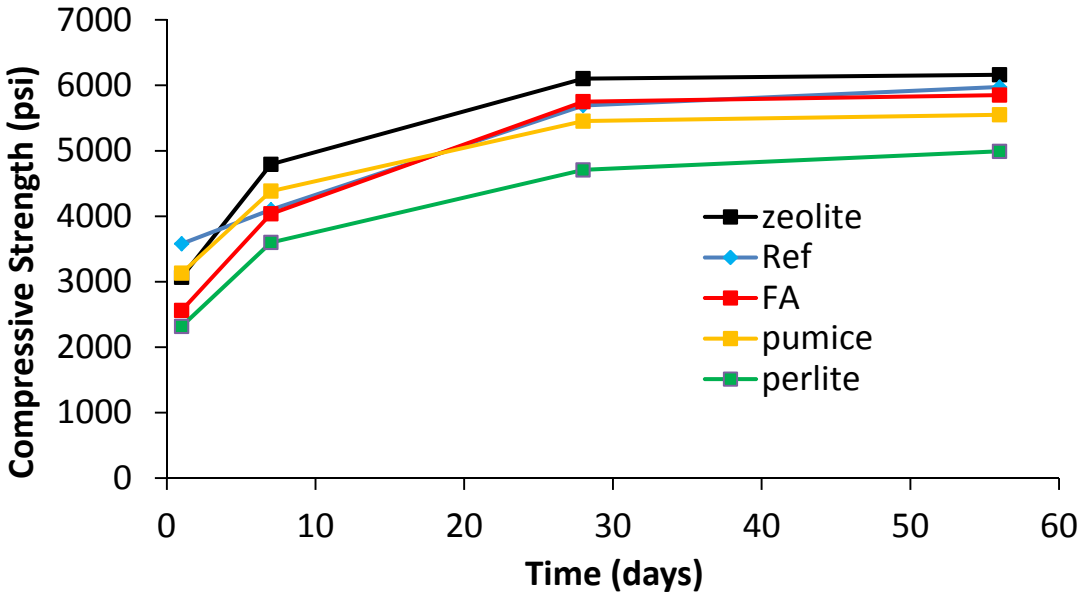

Figure 41. Compressive strength of AEA 2 specimens versus time.

5.9.2 *Modulus of Elasticity*

The average value of the modulus elasticity for both AEA 1 and AEA 2 concrete mixtures are presented in Figure 42. The replacement of cement by PL resulted in a decrease in modulus of elasticity. The results indicates that the incorporation of PM, FA and ZL slightly increased the modulus of elasticity. Also, the effect of type of AEA was found to be negligible.

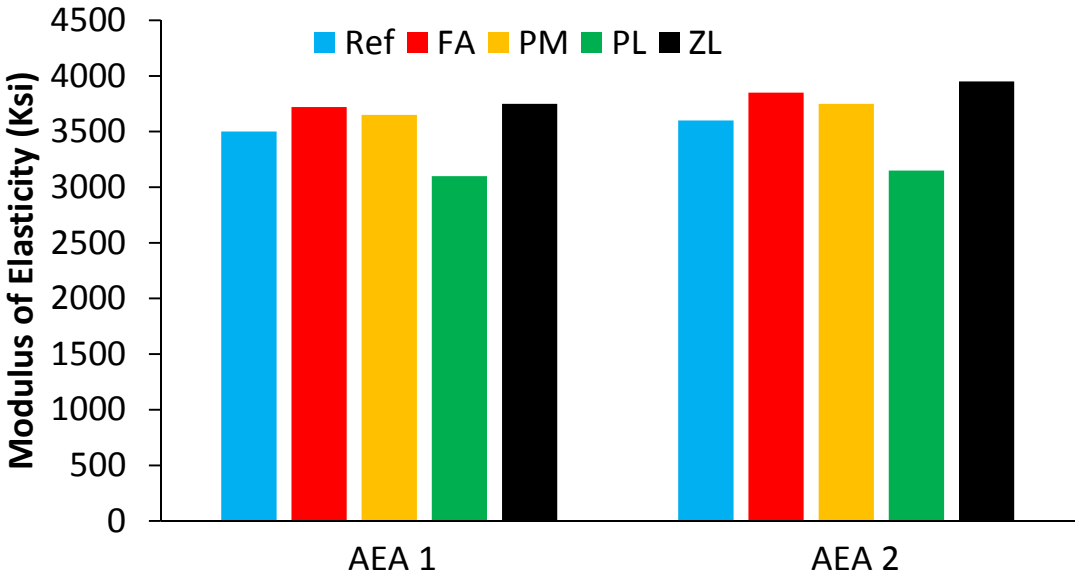

Figure 42. Modulus elasticity of AEA 1 and AEA 2 specimens.

Modulus of elasticity results are compared to the following equations provided by ACI 318 and AASHTO codes for estimating the modulus of elasticity based on the compressive strength:

ACI 318:

$$E = 57000\sqrt{f_c'} \tag{18}$$

AASHTO:

$$E = 33000 W_c^{3/2}\sqrt{f_c'} \tag{19}$$

where E is the modulus of elasticity (in psi for ACI and ksi for AASHTO), W_c is the unit weight of concrete (kcf=1000 pcf) and f'_c is the compressive strength (in psi for ACI and ksi for AASHTO).

Table 14 compares the ACI 318 and AASHTO estimations for the modulus of elasticity based on the compressive strength results at 56 days of age with the value obtained by performing the experimental test. From Table 14, it can be seen that the ACI equation overestimates the modulus of elasticity for all the tested specimens at 56 ages. Similar to the ACI 318 equation, the equation provided by AASHTO overestimates the modulus of elasticity results. However, ACI equation gives more accurate results than AASHTO equation.

It should however be noted that the PL results are significantly different than the other results, both in the experiment as in the prediction, which is not accounted for in neither design code, despite the lower

compressive strength of the mixture. Further investigation is needed on the influence of perlite on the elastic modulus.

Table 14. Comparing the modulus of elasticity measurements with ACI 318 and AASHTO equation

	Mixtures	Experiment (ksi)	ACI 318 (ksi)	AASHTO (ksi)
S1	Ref	3500	3982	4236
	FA	3720	3936	4187
	PL	3100	3805	4251
	PM	3650	3997	4048
	ZL	3750	4174	4439
S2	Ref	3600	4405	4686
	FA	3850	4359	4636
	PL	3150	4246	4516
	PM	3750	4026	4282
	ZL	3950	4474	4758

5.9.3 Splitting Tensile Strength

Figure 43 shows the average values of tensile strength of three specimens. The error bars indicate the standard deviations on the individual values. The results showed that the replacement of cement by ZL led to a slight increase in tensile strength. Also the mixtures with FA and PM slightly outperform the plain cement reference mixture. Remarkably, the tensile strength of the PL mixture is similar to the reference mixture, despite the lower compressive strength.

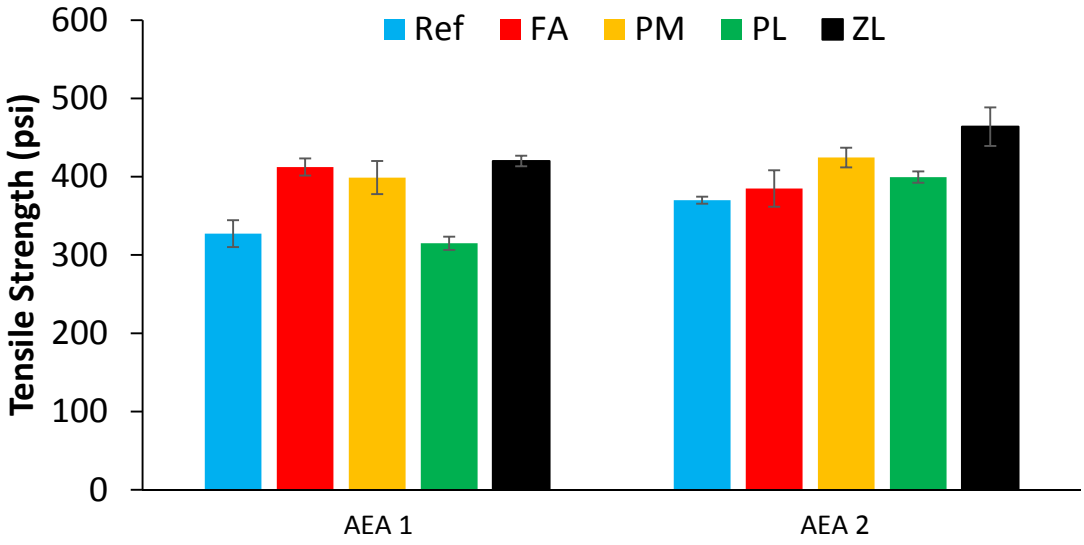

Figure 43. Splitting tensile strength of AEA 1 and AEA 2 series.

5.9.4 Flexural Strength (Modulus of Rupture)

The average values of the flexural strength at 56 days are shown in Figure 44. The results indicate that the addition of ZL had the highest flexural strength in both series of specimens while ref mix showed the lowest value. The inclusion of PM and FA slightly enhance the flexural strength. Also, the mixture with perlite showed slightly higher flexural strength than reference mixture which similar to the observations on the tensile strength. For the AEA 1 specimens, the inclusion of PL, PM, FA and ZL increased the flexural strength by 4%, 22%, 32% and 41% respectively. For the AEA 2 specimens, the addition of PL, PM, FA and ZL increased the flexural strength by 13%, 18%, 12% and 30%, respectively.

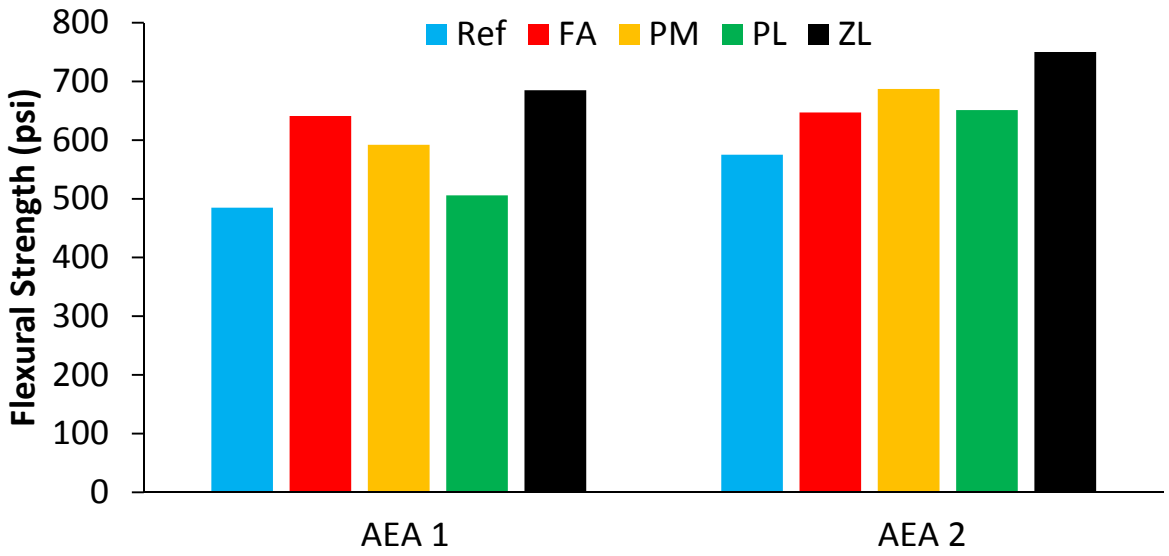

Figure 44. Flexural strength of AEA 1 and AEA 2 series.

5.9.5 Summary

The mixtures with class C fly ash and the pumice showed similar mechanical performance, compared to the reference mixture, except for the strength development, which is slowed down for both SCMs. The zeolite outperforms all mixtures, except at day 1, leading to higher compressive, tensile and flexural strengths compared to the other mixtures. The perlite mixture, however, shows some interesting results. The tensile and flexural strengths are similar to those of the reference mixtures, however the compressive strength is significantly lower. The mixtures with perlite also show a significantly lower modulus of elasticity, not predicted by the ACI and AASHTO design codes despite the lower compressive strength. Further research is needed to investigate whether perlite particles are “softer”, leading to the lower MoE. Softer particles may cause an internal redistribution of stress to the adjacent “harder” particles, potentially explaining the lower compressive strength of the perlite mixtures.

5.10 Air-Void Analysis and Freeze-Thaw Resistance

5.10.1 Cement Pastes

The image of the hardened air content of the paste specimens containing AEA was analyzed using an image editing software to calculate the percentage of entrapped air. Table 15 contains an average of the

percentage of air based on 3 analyzed surfaces from the same cylinder, and Figure 45 presents images from one of the analyzed surface for each SCM and AEA combination. Of the three ASCMs, the paste containing pumice produced the most uniformly distributed air across the cross-section of the samples. Higher air contents were obtained when AEA1 was used than when AEA2 was used (see Table 15), which is to be expected since AEA2 is known to increase slump and therefore cause a reduced retention of the air voids. Overall, pastes containing AEA2 appeared to contain more clustered air compared to pastes containing AEA1. Pastes containing perlite had the lowest entrapped air, which could be due to the better fluidity/fluidity retention (see results presented in 5.2 and 5.3) of the perlite mixtures resulting in better consolidation of the perlite mixtures. Additionally, the lower amount of air within the paste containing perlite could be attributed to the porous structure of the perlite that absorbed the AEAs [4]. The pumice on the other hand reacted well to AEA1 with ideal air voids that are both small and well distributed throughout the specimen whereas with AEA2 the air voids are concentrated more to one side. The high air content of the pumice-AEA1 mixture, coupled with the high standard deviation of that mixture suggest that the air distribution throughout the length of the pumice-AEA1 sample varied more than that of the other cement-ASCM samples. Large pockets of air can be seen in the zeolite samples. This may be due to the negative charge of the zeolites interacting with the air entrainment molecules and disrupting the formation of the stabilized entrained air network.

Table 15. Calculated air contents in hardened cement paste samples containing 1 mL of AEA.

SCM + AEA	Avg. Air content (%)	Standard Deviation
Perlite AEA 2	2.2%	0.23%
Perlite AEA 1	2.7%	0.13%
Pumice AEA 2	3.1%	0.18%
Pumice AEA 1	5.5%	1.25%
Zeolite AEA 2	3.9%	0.41%
Zeolite AEA 1	4.3%	0.30%

.

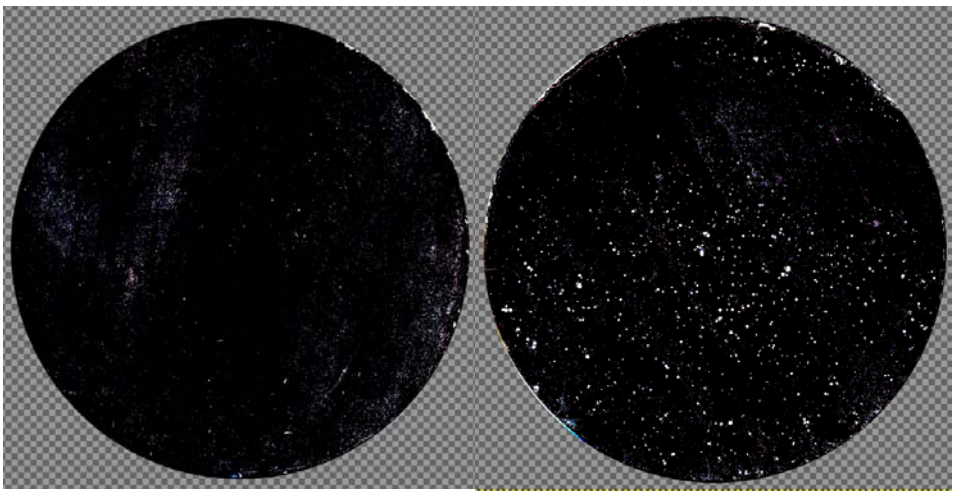

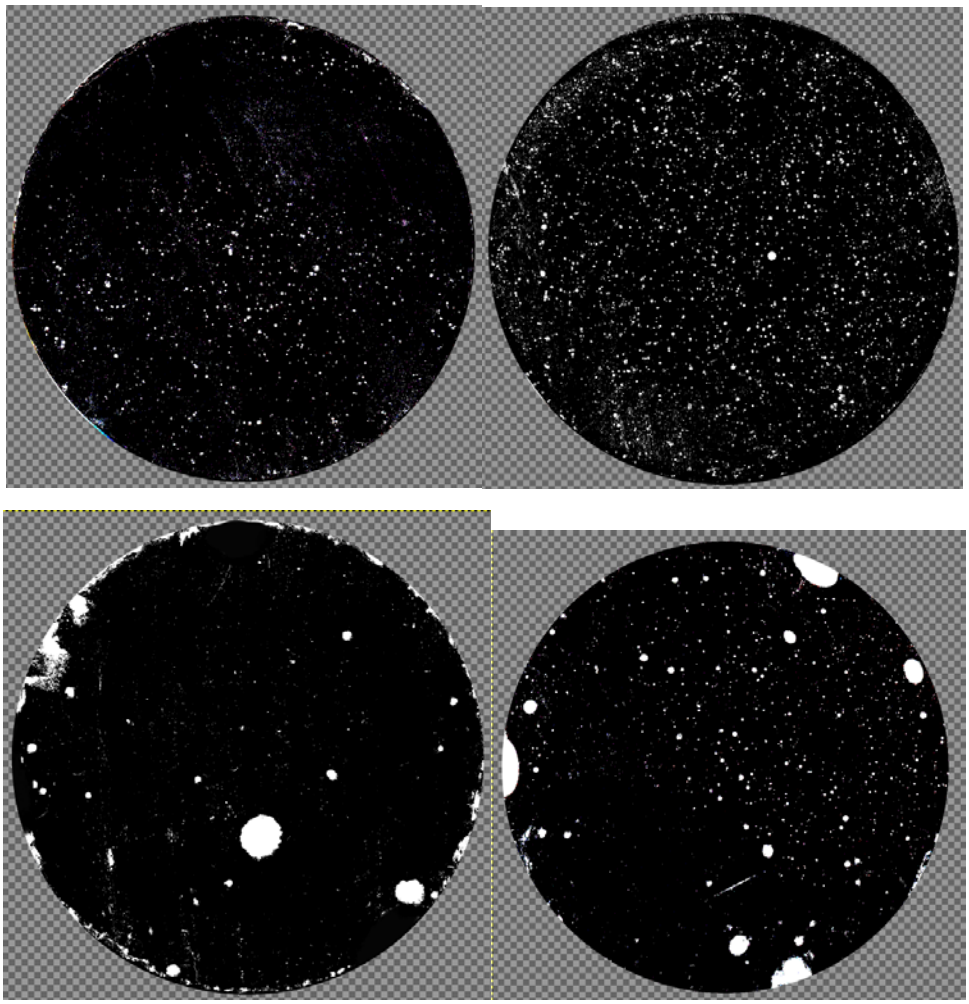

Figure 45. Air void analysis of cement pastes. First row: mixtures containing perlite. Second row: mixtures containing pumice, bottom row: mixture containing zeolite. Left column: AEA 2, right column: AEA 1.

5.10.2 Concrete

Images of the hardened air content of the concrete specimens (see Figure 46) containing AEA 1 was analyzed using the linear transverse method to calculate the percentage of entrapped air in Table 16. All mixtures were proportioned to have an initial air content of 5.5% ± 0.5% (using an air pressure meter). However, it can be seen that the air content of the pumice was considerably less than the targeted value. This could be due to the sorption of the AEA by the pumice over time. Such sorption could result in decreased workability retention (as seen in workability testing of Section 5.4) or increased AEA demand (as seen in the foam index tests in section 5.1). In section 5.6.1, the air content volume over time was measured for the structural concrete mixtures. While a decrease in air content was observed in the pumice concrete mixture, it had a higher air content retention than the zeolite concrete and the perlite concrete. However, the concretes shown in Figure 46 were pavement concretes. Further testing will be done to examine whether the same behavior that is seen in the structural concretes as were seen in the pavement

concretes. If so, this may indicate that the disruption of the air void system from the perlite-AEA interaction occurs over time (>70 minutes after mixing).

Table 16. Measured air contents in the concrete specimens.

SCM + AEA	Average
Perlite AEA 1	8.6%
Pumice AEA 1	2.3%
Zeolite AEA 1	6.4%

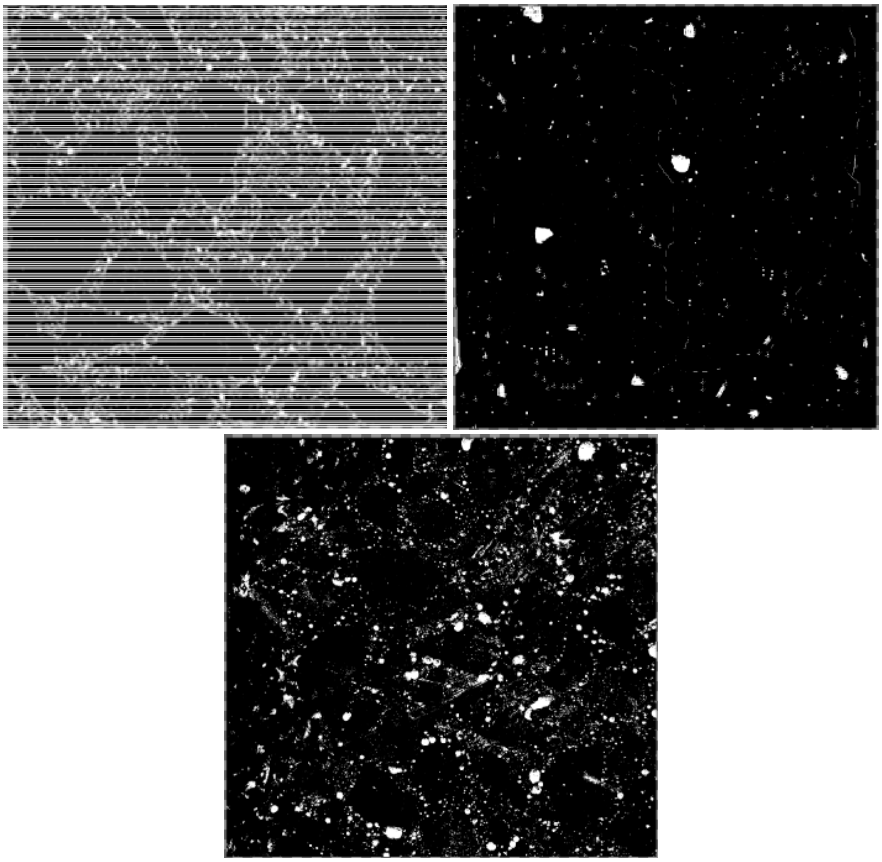

Figure 46: Air void analysis of concrete. Mixtures containing perlite, pumice, and zeolite (respectively).

5.11 Non-Destructive Test Results Related to Corrosion Resistance

5.11.1 Surface and Bulk Resistivity

The surface resistivity was performed at 56 days of age. A correction factor equal to 1.1 was applied to the measurements for compensating the effect of lime curing according to AASHTO TP-95. Figure 47 shows the average value of surface resistivity for AEA 1 and AEA 2 specimens. As can be seen, the reference specimen had the lowest value of resistivity.

There was no significant difference between the resistivity results of the specimens containing PL, PM and FA. According to Table 7, all the specimens except ZL-mix in both series of specimens are classified

in a high corrosion rate zone. As shown, the addition of ZL led to a significant increase in resistivity of concrete specimens which, for the AEA 1 series, were classified in Low to moderate corrosion rate.

The average value of bulk resistivity for AEA 1 and AEA 2 specimens are presented in Figure 48. The results are in a good agreement with surface resistivity test. The ZL-mixture shows the highest value of bulk resistivity. The incorporation of all mineral admixtures (PL, PM and FA) led to an increase in the value of bulk resistivity compared with Ref mix. There was no significant difference in bulk resistivity of the PL, PM mixture and the mixtures made with FA. However, the variation in the results between two series of the mixes implied that the effect of air-entrainment admixture can be considered as an influential parameter.

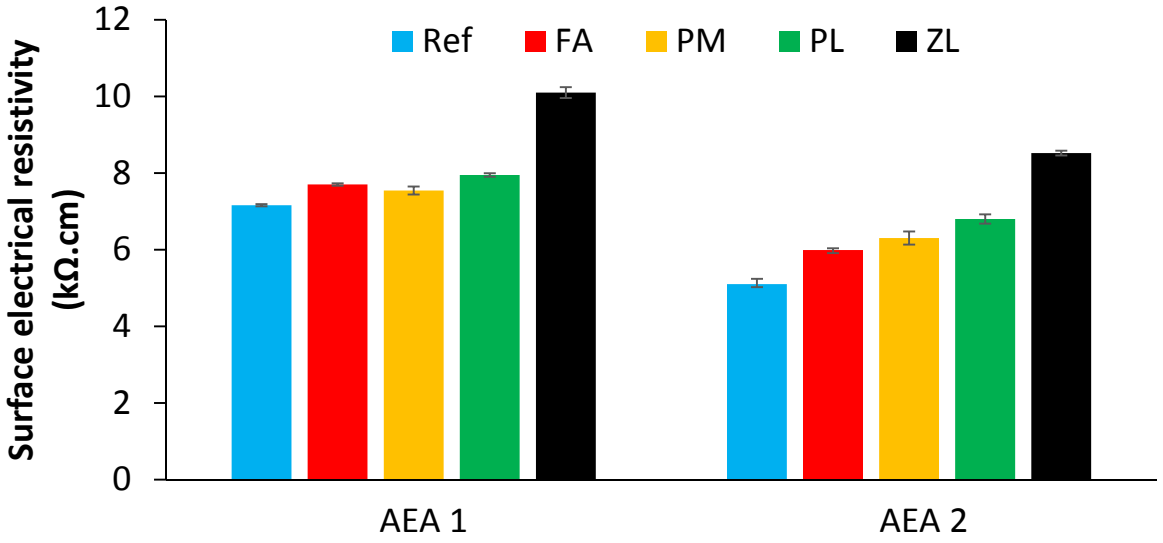

Figure 47. Surface resistivity results AEA 1 and AEA 2 specimens.

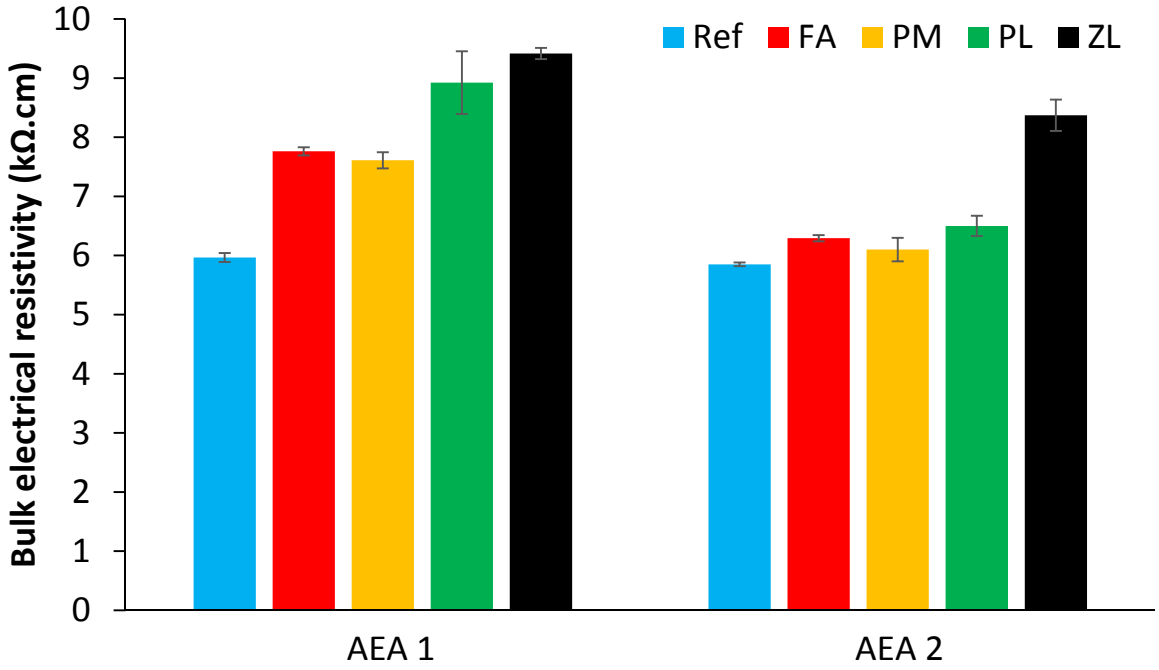

Figure 48. Bulk resistivity results AEA 1 and AEA 2 specimens.

5.11.2 Permeable Voids Volume and Absorption

The average value of volume of permeable voids (VPV) for both AEA 1 and AEA 2 series are presented in Figure 49. There was no significant difference in VPV of the mixtures containing SCMs compared with the reference. The results of absorption are presented in Figure 50. The mixtures containing SCMs had a slightly higher absorption than the reference mixture. However no substantial difference was observed between mixtures containing SCMs.

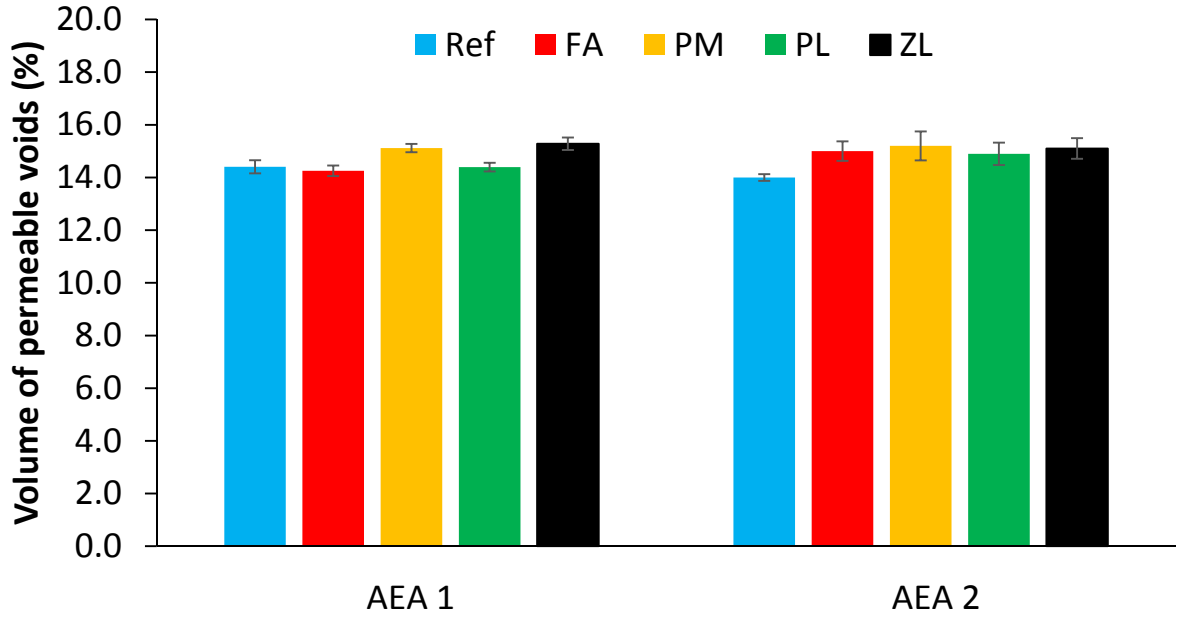

Figure 49. Volume of permeable voids results AEA 1 and AEA 2 specimens.

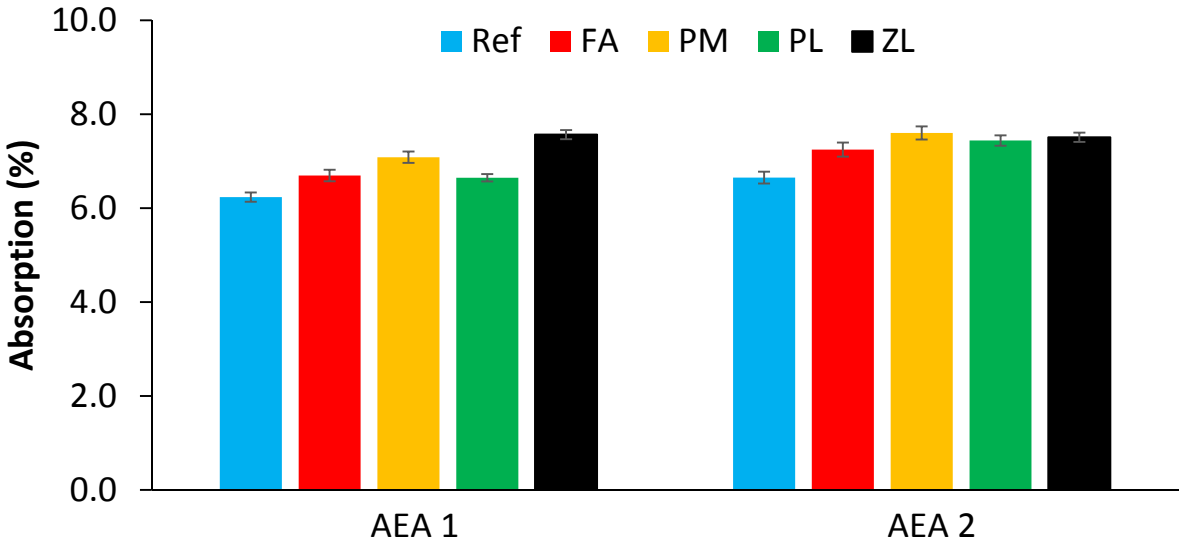

Figure 50. Absorption results AEA 1 and AEA 2 specimens.

6 Conclusions

6.1 General Conclusions

The experimental study herein described was conducted aiming to evaluate the compatibility of two types of air-entrainment with selected types of alternative SCMs. In addition, the influence of selected alternative SCMs on key fresh and hardened properties of concrete designated for the construction of bridge and tunnel infrastructure was studied.

The following conclusions are highlighted:

AEA demand increases when pumice, zeolite, or perlite is used as to replace 25% cement (by mass). AEA demand depends on the type of ASCM used, and the AEA demand to produce a stable foam in the plain pumice suspension was considerably larger than that of the plain zeolite suspension and plain perlite suspension. However, when an ASCM is added to a cement suspension, regardless of whether the ASCM was perlite, pumice, or zeolite, similar relative foam indices were obtained for the ASCM-cement suspension.

For plain cement paste and pastes with 20% fly ash or 20% perlite (by vol.), the same saturation dosage (0.3 % by mass of binder) was obtained. The admixture saturation dosage for pumice and zeolite was higher.

The rheological properties of the pastes were followed with time to investigate the workability retention. It was found that the inclusion of pumice and zeolite led to an increase in yield stress and plastic viscosity with time, compared to the mixtures with perlite or fly ash, or the plain cement mixtures, regardless of temperature. In addition, the results indicated that the incorporation of perlite and fly ash reduces the yield stress and viscosity with time compared to the plain cement mixture.

The effect of different temperatures on yield stress and viscosity evolution with time was studied. As expected, both yield stress and viscosity increase faster with increasing temperature, however for the mixtures with plain cement, fly ash and perlite, no substantial difference in workability retention is noticed at each temperature.

The effect of two different types of AEA on the air content and stability of air void system was studied. Regardless of type of AEA, the mixtures containing pumice and perlite have the most stable air-void system among all tested SCMs after 70 minutes, while a dramatic decrease in air content was observed for the mixture containing fly ash. Also the results indicated that AEA2 has more stable air regardless of the type of SCMs used in mix.

The workability retention of the concrete mixtures was studied. According to the results, the replacement of cement by perlite and fly ash enhances the workability retention while the high slump loss can be observed for zeolite and pumice mixes. The rheological analysis indicated that the mixtures with pumice and zeolite have a larger increase of yield stress and plastic viscosity with time, compared to the mixtures with perlite or fly ash, or the plain cement mixtures. It was observed that the inclusion of perlite and fly ash reduces the yield stress and viscosity with time compared to the plain cement mixture. The obtained rheological results were in good agreement with workability retention values obtained by the slump test.

The results of the calorimetry analysis revealed that the inclusion of zeolite accelerated the hydration reaction significantly and released almost the same cumulative heat compared to the plain cement paste,

while pumice accelerated the reaction slightly during the first 12 hours of the test. Perlite has the lowest heat flow among all SCMs which implied a slower hydration reaction. The hydration reaction was also delayed when including fly ash and pumice.

Hardened properties of concrete specimens containing different SCMs were studied. The early age test results showed that the incorporation of any SCM led to a decrease of 1-day concrete compressive strength. It was observed that the addition of zeolite significantly increased the early-age compressive strength beyond 1 day which is due to the faster hydration of the zeolite particles and the large and highly reactive surface area. zeolite-mix showed the highest compressive strength at all the ages except at one-day age. However the addition of pumice and fly ash showed almost the same strength values as the reference mix at later ages. No significant difference was observed in modulus of elasticity of the specimens made with different type of SCMs. The results showed that the replacement of cement by zeolite led to a slight increase in tensile strength. Also there was no significant improvement between the mixes containing different SCMs. The results indicated that the addition of zeolite had the highest flexural strength in both series of specimens while ref mix showed the lowest value. The inclusion of pumice and fly ash slightly enhance the flexural strength. The tensile and flexural strengths of the PL mixtures are similar to those of the reference mixtures, however the compressive strength and modulus of elasticity are significantly lower.

Both surface and bulk resistivity were measured as an indication of durability. The plain-cement mixture showed the lowest value of resistivity. However, there was no significant difference between the resistivity results of the specimens containing perlite, pumice and fly ash. The results revealed that all the specimens except zeolite-mix in the AEA 1 series of specimens are classified in a high corrosion rate zone. The addition of zeolite led to a significant increase in resistivity of concrete specimens which were classified in low to moderate corrosion rate. In addition, the incorporation of all SCMs (perlite, pumice and fly ash) led to an increase in the value of bulk resistivity compared with the reference mixture. There was no significant difference in bulk resistivity of the perlite, pumice mixture and the mixtures made with fly ash. However, the variation in the results between two series of the mixes implied that the effect of air-entrainment admixture can be considered as an influential parameter.

Air void analysis of hardened cement paste and hardened concrete samples were conducted. For the paste samples, pastes containing perlite had the lowest entrapped air, which could be due to the better fluidity/fluidity retention of the perlite mixtures resulting in better consolidation of the perlite mixtures and/or sorption of AEA by the perlite. Large pockets of air were evident in the zeolite samples that were not seen in the other pastes. With respect to the concrete samples, the air content of the pumice containing concrete was lower than the other mixtures and it was considerably less than initial air content value.

The inclusion of SCMs didn't cause any significant improvement in enhancing the volume of permeable voids neither in absorption of concrete specimens compared with the reference mixture. From a corrosion point of view, all SCMs tested appear to be viable materials for the incorporation in structural concrete.

Table 17 summarizes the performance of the alternative SCMs (and fly ash), compared to the plain cement mixtures for mixtures intended for structural applications. The tested Class C fly ash is advantageous for workability retention, but problems arise in keeping the amount of air in the concrete. Perlite appears to be a suitable material regarding the fresh properties, but a reduction in heat of hydration, compressive strength and E-modulus may reduce its implementation for structural applications.

Mixtures with pumice perform very similar to the reference mixture, apart from the SP demand and a decrease in workability retention. The zeolite performs very well in the hardened state, but has a very high admixture demand and an inferior workability retention.

Table 17. Summary of performance of SCMs-cement mixtures compared to plain cement mixtures. "/" indicates no significant change, "+" and "-" represent a positive or negative influence, respectively. Double symbols indicate a strong influence.

	Class C fly ash	Perlite	Pumice	Zeolite
AEA / SP demand	/	/	-	- -
Air content retention	- -	/	/	/
Workability retention	+	+	- -	- -
Mechanical Properties (at 56 days)	/	- -	/	+
Corrosion resistance	/	/	/	+

6.2 Recommendations to Concrete Producers

Searching the perfect alternative supplementary cementitious material is a complicated task. The new material must perform similarly or better than the reference mix designs in terms of admixture compatibility, workability, mechanical properties and durability. From this research project, it can be concluded that each of the three investigated alternatives for fly ash has at least one disadvantage.

Incorporating perlite into concrete mixtures is similar to using fly ash. Workability is slightly improved showing adequate retention, the admixture dosages are similar and the perlite has the advantage over fly ash to keep the air content more stable over time, in the fresh state. However, the studied perlite showed a mild reduction in compressive strength and in elastic modulus, without affecting tensile properties. Using perlite in applications where the stiffness of the concrete is a crucial parameter (such as bridge girders), must be done with the necessary care, especially from a design point of view.

The performance of the mixtures with pumice in the hardened state is not different than mixtures with fly ash. The strength development needs some additional time, compared to plain cement mixtures, but at later ages, the strength, elastic modulus and durability of these mixtures is similar to plain cement mixtures or mixtures with fly ash. However, in the fresh state, the slight increase in admixture demand and the worse workability retention may reduce the application potential of pumice. Especially in applications with long transportation or waiting times, the use of pumice may show disadvantages. However, in the pre-cast industry, where workability retention is of lesser importance, pumice can be a good alternative for cement or fly ash. Furthermore, the workability retention may be improved by employing different WRA.

The zeolite delivers the best performance in terms of mechanical properties and corrosion resistance, even compared to the reference, plain cement mixture. But the workability retention and admixture demand pose a severe limitation on the application of zeolite. The studied zeolite can be a useful material in applications where workability is of no significant importance. In applications with zero-slump concrete, or in construction procedures that require extreme consolidation energy (e.g. centrifuging high-strength concrete), zeolites can be used to enhance the mechanical properties and durability.

6.3 Future Work

For the materials studied in this project, future research is needed to find cost-effective and environment-friendly solutions to reduce the "weaknesses" of each of the materials. Each material has shown promising results for applications in transportation infrastructure, but full-scale implementation can only be done when the observed negative points are solved. More experiments need to be performed to test compatibility issues between the materials and other chemical admixtures. For example, how do the pumice and zeolite perform in presence of a high slump-retention admixture?

More generally, research on alternative SCMs is useful to reduce cost, increase recycling and reduce carbon gas emissions. Large scale research is needed to generate a database of typical physical and chemical properties, which vary for each used material, and link these properties to the performance of concrete in fresh and hardened state. With this database, the most critical chemical and physical properties can be identified and their influence investigated, to create practical guidelines concerning the testing, acceptance and use of supplementary cementitious materials in practice. These guidelines will simplify the day-to-day or delivery-to-delivery quality control of the materials and help concrete producers in assessing or even predicting changes in concrete performance with each new material, or even with each new delivery. In this way, trial and error or out-of-spec concrete deliveries will be reduced, resulting in significant cost savings, not only for the concrete producer, but also for infrastructure owners and society.

7 References

[1] Klieger, P., D. Stark, and W. Teske. 1978. The influence of environment and materials on d-cracking. Final report (October). Skokie, Ill.: Construction Technology Laboratories.

[2] Pigeon, M., and M. Plante. 1989. Air-void stability part I: Influence of silica fume and other parameters. ACI Journal 86 (5):482-90.

[3] M. Rotella, G. Simandl, Marilla Perlite – Volcanic Glass Occurrence, British Columbia, Canada, Geological Fieldwork 2002, Paper 2003-1.

[4] F. Bektas, L. Turanli, P.J.M. Monteiro - Use of Perlite Powder to suppress alkali-silica reaction, Cement & Concrete Research 35 (2005) 2014-2017.

[5] A. Ray, R. Sriravindrarajah, J.P. Guerbois, P. S. Thomas, S. Border, H. N. Ray, J. Haggman and P. Joyce, Evaluation of Waste Perlite Fines in the Production of Construction Material, Journal of Thermal Analysis and Calorimetry 88 (2007) 1, 279-283.

[6] T.K. Erdem, C. Meral, M. Tokyay, T.Y. Erdogan, Use of perlite as a pozzolanic addition in producing blended cements, Cement & Concrete Composites 29 (2007) 13–21.

[7] ACI Committee 232, Report on the Use of Raw or Processed natural Pozzolans in Concrete (ACI 232.1R-12). Farmington Hills, MI: American Concrete Institute, 2012.

[8] K.M.A. Hossain, M. Lachemi, Performance of volcanic ash and pumice based blended cement concrete in mixed sulfate environment, Cement and Concrete Research 36 (2006) 1123-1133.

[9] K.M.A. Hossain, Blended cement using volcanic ash and pumice, Cement and Concrete Research 33 (2003) 1601-1605.

[10] K.M.A. Hossain, Potential Use of Volcanic Pumice as a Construction Material, ASCE Journal of Materials in Civil Engineering 16 (2004) 573-577.

[11] R. Snellings, G. Mertens, J. Elsen, Supplementary Cementitious Materials, Reviews in Mineralogy & Geochemistry 74 (2012) 211-278.

[12] K.M.A. Hossain, Chloride induced corrosion of reinforcement in volcanic ash and pumice based blended concrete, Cement and Concrete Composites 27 (2005) 381-390.

[13] Mielenz, R.C., Witte, L.P. and Glantz, O.J., Effect of Calcination on Natural Pozzolana, Symposium on Use of Pozzolanic Materials in Mortars and Concretes, STP-99, American Society for Testing and Materials, 1950, 43-91.

[14] R. Pabalan, P. Bertetti, Cation-exchange properties of natural zeolites, Reviews in Mineralogy and Geochemistry 45 (2001) 1 453-518.

[15] T. Perraki, E. Kontori, E., S. Tsivilis, G. Kakali, The effect of zeolite on the properties and hydration of blended cements, Cement and Concrete Composites 32 (2010) 129-133.

[16] M. Rosell-Lam, E. Villar-Cocina, M. Frias, Study on the pozzolanic properties of a natural Cuban zeolitic rock by conductometric method: Kinetic parameters, Construction and Building Materials 25 (2011) 644-650.

[17] B. Ahmadi, M. Shekarchi, Use of natural zeolite as a supplementary cementitious material, Cement and Concrete Composites, 32 (2010) 134-141.

[18] C. Bilim, Properties of cement mortars containing clinoptilolite as a supplementary cementitious material, Construction and Building Materials 25 (2011) 3175-3180.

[19] V. Lilkov, I. Rostovsky, O. Petrov, Physical and mechanical characteristics of cement mortars and concretes with addition of clinoptilolite from Beli Plast deposit (Bulgaria), silica fume and fly ash, Clay Minerals 46 (2011) 213-223.

[20] T. Perraki, T., G. Kakali, E. Kontori, Characterization and pozzolanic activity of thermally treated zeolite. Journal of Thermal Analysis and Calorimetry, 82 (2005) 1 109-113.

[21] E. Liebig, E. Althaus, Pozzolanic Activity of Volcanic Tuff and Suevite: Effects of Calcination, Cement and Concrete Research 28 (1998) 4 567-575.

[22] USGS, 2011 Mineral Yearbook Zeolites (Advance Release) http://minerals.usgs.gov/minerals/pubs/commodity/zeolites/myb1-2011-zeoli.pdf

[23] Cano, R. (2013). Evaluation of Natural Pozzolans as Replacements for Class F Fly Ash in Portland Cement Concrete. Department of Civil, Architectural and Environmental Engineering. Austin, Texas, University of Texas at Austin. M.Sc. Thesis.

[24] Wallevik JE, Rheology of particle suspensions - Fresh concrete, mortar and cement paste with various types of lignosulfonates [Doctoral thesis]. Trondheim, Norway: The Norwegian University of Science and Technology (NTNU); 2003.

[25] Chini AR, Muszynski, L.C., and Hicks, J. Determination of acceptance permeability characteristics for performance-related specifications for portland cement concrete. final report submitted to Florida Department of Transportation2003. p. 116-8.

[26] Resipod Family Operating instructions, concrete durability testing. Proceq; 2013.

[27] Research Report Cement Concrete and Aggregates Australia, Chloride Resistance of Concrete. 2009.

[28] Pomeroy D. Concrete durability: From basic research to practical reality. ACI special publication. 1989;SP- 100:111 -31.

[29] Whiting D, Dziedzic, W. Effect of second-generation high range water-reducers on durability and other properties of hardened concrete. 1990;in ACI special publication SP-122:81-104.

[30] Pedersen KHJ, A. D., Skjøth-Rasmussen, M. S., Dam-Johansen, K. A review of the interference of carbon containing fly ash with air entrainment in concrete. Progress in Energy and Combustion Science. 2008;34(2):135-54.

[31] Freeman E, Gao, Y.M., Hurt, R., Suuberg, E. Interactions of carbon-containing fly ash with commercial air-entraining admixtures for concrete. Fuel. 1997;76(8):761-5.

[32] Hill RL, Shondeep, L.S., Rathbone, R. F., Hower, J.C. An examination of fly ash carbon and its interactions with air entraining agent. Cement and Concrete Research. 1997;27(2):193-204.

[33] Lin KL, Chang, W.C., Lin, D.F., Luo, H.L., Tsai, M.C. Effects of nano-SiO(2) and different ash particle sizes on sludge ash-cement mortar. J Environ Manage. 2008;88(4):708–14.

[34] Björnström J, Martinelli, A., Matic, A., Börjesson, L., Panas,I. Accelerating effects of colloidal nano-silica for beneficial calcium–silicate–hydrate formation in cement. Chemical Physics Letters. 2004;392(1–3):242-8.

[35] Ghafari E, Costa, H., Júlio, E, Portugal, A., Durães, L. The effect of nanosilica addition on flowability, strength and transport properties of ultra high performance concrete. Materials & Design 2014;59:1-9.